Pathway Analysis Report

Gene

This report contains the pathway analysis results for the submitted sample 'Gene'. Analysis was performed against Reactome version 68 on 10/04/2019. The web link to these results is:

https://reactome.org/PathwayBrowser/#/ANALYSIS=MjAxOTA0MTAxMDU2NDZfODQzNg%3D%3D

Please keep in mind that analysis results are temporarily stored on our server. The storage period depends on usage of the service but is at least 7 days. As a result, please note that this URL is only valid for a limited time period and it might have expired.

Table of Contents

1. Introduction

Reactome is a curated database of pathways and reactions in human biology. Reactions can be considered as pathway 'steps'. Reactome defines a 'reaction' as any event in biology that changes the state of a biological molecule. Binding, activation, translocation, degradation and classical biochemical events involving a catalyst are all reactions. Information in the database is authored by expert biologists, entered and maintained by Reactome's team of curators and editorial staff. Reactome content frequently cross-references other resources e.g. NCBI, Ensembl, UniProt, KEGG (Gene and Compound), ChEBI, PubMed and GO. Orthologous reactions inferred from annotation for Homo sapiens are available for 17 non-human species including mouse, rat, chicken, puffer fish, worm, fly, yeast, rice, and Arabidopsis. Pathways are represented by simple diagrams following an SBGN-like format.

Reactome's annotated data describe reactions possible if all annotated proteins and small molecules were present and active simultaneously in a cell. By overlaying an experimental dataset on these annotations, a user can perform a pathway over-representation analysis. By overlaying quantitative expression data or time series, a user can visualize the extent of change in affected pathways and its progression. A binomial test is used to calculate the probability shown for each result, and the p-values are corrected for the multiple testing (Benjamini–Hochberg procedure) that arises from evaluating the submitted list of identifiers against every pathway.

To learn more about our Pathway Analysis, please have a look at our relevant publications:

Fabregat A, Sidiropoulos K, Garapati P, Gillespie M, Hausmann K, Haw R, … D'Eustachio P (2016). The reactome pathway knowledgebase. Nucleic Acids Research, 44(D1), D481–D487. https://doi.org/10.1093/nar/gkv1351.

Fabregat A, Sidiropoulos K, Viteri G, Forner O, Marin-Garcia P, Arnau V, … Hermjakob H (2017). Reactome pathway analysis: a high-performance in-memory approach. BMC Bioinformatics, 18.

2. Properties

- This is an **expression** analysis: The numbers are used to produce a scaled coloured overlay over Reactome pathway diagrams, as a means to visualize relative expression levels. Note that the numeric values do not have to be expression data, for instance by using gene association scores the same analysis can be used to visualize genotyping results.

- 337 out of 461 identifiers in the sample were found in Reactome, where 1601 pathways were hit by at least one of them.

- All non-human identifiers have been converted to their human equivalent.

- IntAct interactors were included to increase the analysis background. This greatly increases the size of Reactome pathways, which maximises the chances of matching your submitted identifiers to the expanded pathway, but will include interactors that have not undergone manual curation by Reactome and may include interactors that have no biological significance, or unexplained relevance.

- This report is filtered to show only results for species 'Homo sapiens' and resource 'all resources'.

- The unique ID for this analysis (token) is MjAxOTA0MTAxMDU2NDZfODQzNg%3D%3D. This ID is valid for at least 7 days in Reactome's server. Use it to access Reactome services with your data.

3. Genome-wide overview
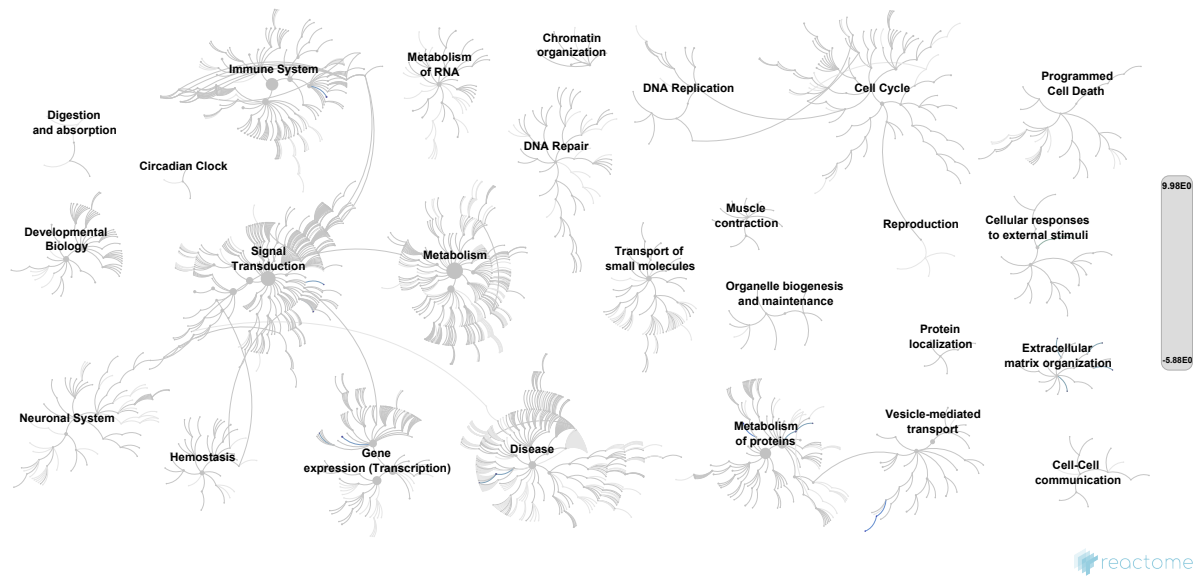
This figure shows a genome-wide overview of the results of your pathway analysis. Reactome pathways are arranged in a hierarchy. The center of each of the circular "bursts" is the root of one top-level pathway, for example "DNA Repair". Each step away from the center represents the next level lower in the pathway hierarchy. The color code denotes over-representation of that pathway in your input dataset. Light grey signifies pathways which are not significantly over-represented.

4. Most significant pathways

The following table shows the 25 most relevant pathways sorted by p-value.

Pathway name	Entities				Reactions	
	found	ratio	p-value	FDR*	found	ratio
Nuclear Receptor transcription pathway	13 / 101	0.005	1.05e-04	0.184	2 / 2	1.65e-04
Interleukin-4 and Interleukin-13 signaling	30 / 365	0.018	4.71e-04	0.412	16 / 46	0.004
Laminin interactions	6 / 33	0.002	0.001	0.786	14 / 15	0.001
Antagonism of Activin by Follistatin	6 / 14	6.99e-04	0.002	0.786	2 / 2	1.65e-04
Anchoring fibril formation	4 / 15	7.49e-04	0.002	0.806	4 / 4	3.30e-04
Defective B3GALTL causes Peters-plus syndrome (PpS)	6 / 39	0.002	0.003	0.806	1 / 1	8.25e-05
Metallothioneins bind metals	6 / 39	0.002	0.003	0.806	14 / 27	0.002
O-glycosylation of TSR domain-containing proteins	6 / 41	0.002	0.004	0.894	2 / 2	1.65e-04
Collagen chain trimerization	6 / 44	0.002	0.006	0.966	5 / 28	0.002
Response to metal ions	6 / 47	0.002	0.008	0.966	14 / 31	0.003
Regulation of FZD by ubiquitination	5 / 34	0.002	0.008	0.966	6 / 6	4.95e-04
Microtubule-dependent trafficking of connexons from Golgi to the plasma membrane	4 / 22	0.001	0.009	0.966	1 / 2	1.65e-04
Transport of connexons to the plasma membrane	4 / 23	0.001	0.01	0.966	1 / 3	2.48e-04
Collagen degradation	7 / 76	0.004	0.022	0.966	12 / 34	0.003
FOXO-mediated transcription of oxidative stress, metabolic and neuronal genes	14 / 132	0.007	0.023	0.966	32 / 34	0.003
Diseases associated with O-glycosylation of proteins	7 / 79	0.004	0.026	0.966	2 / 9	7.43e-04
Post-chaperonin tubulin folding pathway	4 / 35	0.002	0.039	0.966	9 / 9	7.43e-04
O-linked glycosylation	12 / 170	0.008	0.047	0.966	5 / 28	0.002
Activation of AMPK downstream of NMDARs	7 / 74	0.004	0.054	0.966	3 / 3	2.48e-04
Assembly of collagen fibrils and other multimeric structures	6 / 74	0.004	0.054	0.966	23 / 26	0.002
Crosslinking of collagen fibrils	3 / 24	0.001	0.057	0.966	12 / 13	0.001
Molecules associated with elastic fibres	4 / 40	0.002	0.058	0.966	6 / 10	8.25e-04
TGFBR2 MSI Frameshift Mutants in Cancer	1 / 2	9.98e-05	0.07	0.966	1 / 1	8.25e-05

Pathway name	Entities				Reactions	
	found	ratio	p-value	FDR*	found	ratio
VEGF ligand-receptor interactions	6 / 27	0.001	0.075	0.966	3 / 4	3.30e-04
VEGF binds to VEGFR leading to receptor dimerization	6 / 27	0.001	0.075	0.966	2 / 3	2.48e-04

* False Discovery Rate

5. Pathways details

For every pathway of the most significant pathways, we present its diagram, as well as a short summary, its bibliography and the list of inputs found in it.

1.   Nuclear Receptor transcription pathway (R-HSA-383280)
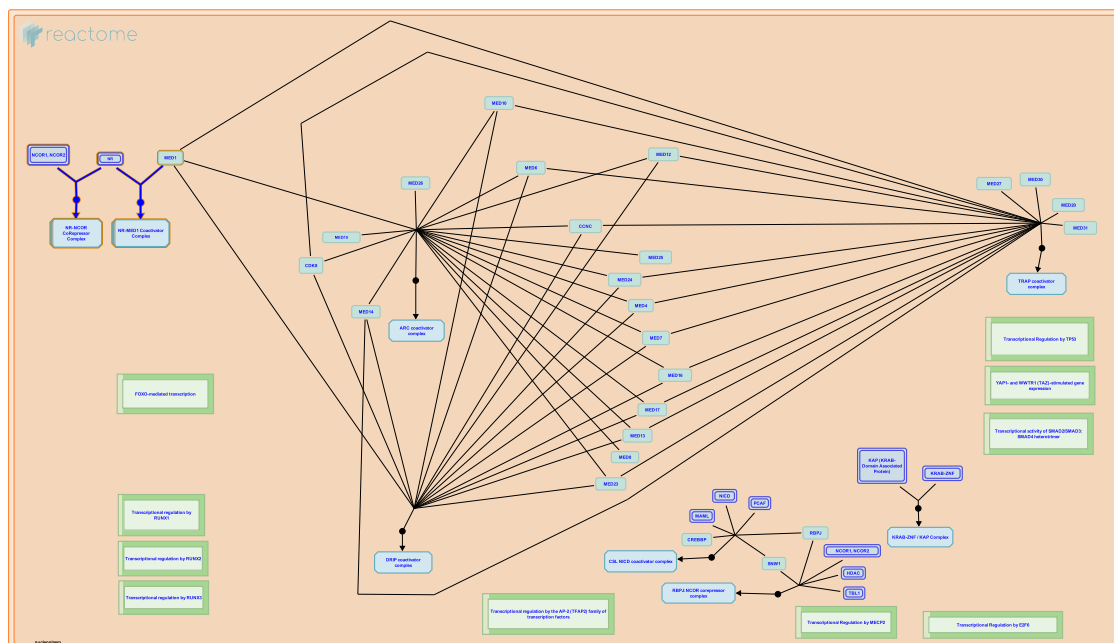
A classic example of bifunctional transcription factors is the family of Nuclear Receptor (NR) proteins. These are DNA-binding transcription factors that bind certain hormones, vitamins, and other small, diffusible signaling molecules. The non-liganded NRs recruit specific corepressor complexes of the NCOR/SMRT type, to mediate transcriptional repression of the target genes to which they are bound. During signaling, ligand binding to a specific domain the NR proteins induces a conformational change that results in the exchange of the associated CoR complex, and its replacement by a specific coactivator complex of the TRAP / DRIP / Mediator type. These coactivator complexes typically nucleate around a MED1 coactivator protein that is directly bound to the NR transcription factor.

A general feature of the 49 human NR proteins is that in the unliganded state, they each bind directly to an NCOR corepressor protein, either NCOR1 or NCOR2 (NCOR2 was previously named "SMRT"). This NCOR protein nucleates the assembly of additional, specific corepressor proteins, depending on the cell and DNA context. The NR-NCOR interaction is mediated by a specific protein interaction domain (PID) present in the NRs that binds to specific cognate PID(s) present in the NCOR proteins. Thus, the human NRs each take part in an NR-NCOR binding reaction in the absence of binding by their ligand.

A second general feature of the NR proteins is that they each contain an additional, but different PID that mediates specific binding interactions with MED1 proteins. In the ligand-bound state, NRs each take part in an NR-MED1 binding reaction to form an NR-MED1 complex. The bound MED1 then functions to nucleate the assembly of additional specific coactivator proteins, depending on the cell and DNA context, such as what specific target gene promoter they are bound to, and in what cell type.

The formation of specific MED1-containing coactivator complexes on specific NR proteins has been well-characterized for a number of the human NR proteins (see Table 1 in (Bourbon, 2004)). For example, binding of thyroid hormone (TH) to the human TH Receptor (THRA or THRB) was found to result in the recruitment of a specific complex of Thyroid Receptor Associated Proteins - the TRAP coactivator complex - of which the TRAP220 subunit was later identified to be the Mediator 1 (MED1) homologue.

Similarly, binding of Vitamin D to the human Vitamin D3 Receptor was found to result in the recruitment of a specific complex of D Receptor Interacting Proteins - the DRIP coactivator complex, of which the DRIP205 subunit was later identified to be human MED1.

References

Edit history

Date	Action	Author
2008-11-20	Authored	Caudy M
2008-12-03	Created	Caudy M
2009-05-27	Edited	Caudy M
2009-08-29	Reviewed	Freedman LP
2019-03-13	Modified	Weiser D

Entities found in this pathway (4)

Input	UniProt Id	#FC
PPARG	P37231	1.03
NR4A1	P22736	1.34
NR4A3	Q92570-1, Q92570-2	2.11
NR3C1	P04150-1, P04150-2, P04150-3, P04150-4, P04150-5, P04150-6, P04150-7, P04150-8, P04150-9	-1.01e+00

2. Interleukin-4 and Interleukin-13 signaling (R-HSA-6785807)
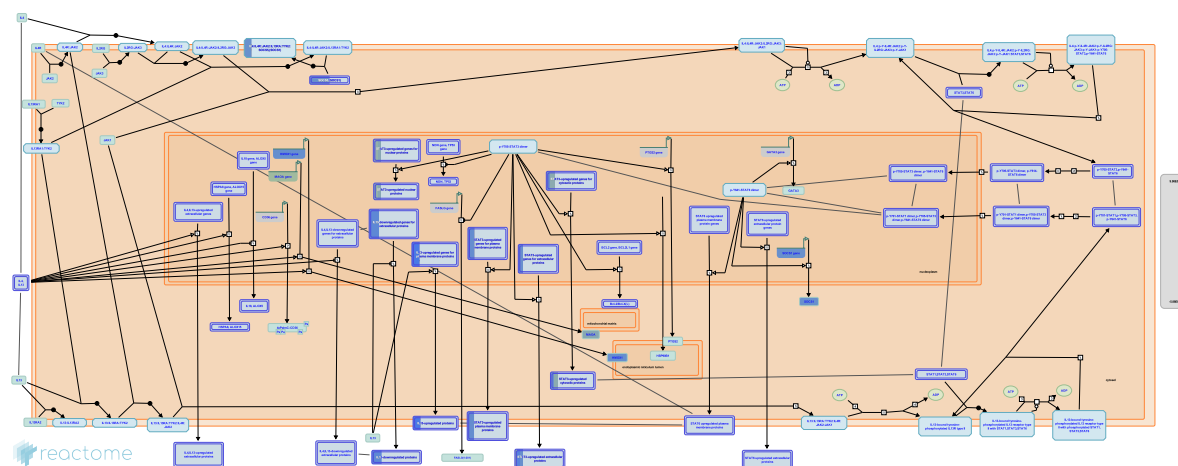
Interleukin-4 (IL4) is a principal regulatory cytokine during the immune response, crucially important in allergy and asthma (Nelms et al. 1999). When resting T cells are antigen-activated and expand in response to Interleukin-2 (IL2), they can differentiate as Type 1 (Th1) or Type 2 (Th2) T helper cells. The outcome is influenced by IL4. Th2 cells secrete IL4, which both stimulates Th2 in an autocrine fashion and acts as a potent B cell growth factor to promote humoral immunity (Nelms et al. 1999).

Interleukin-13 (IL13) is an immunoregulatory cytokine secreted predominantly by activated Th2 cells. It is a key mediator in the pathogenesis of allergic inflammation. IL13 shares many functional properties with IL4, stemming from the fact that they share a common receptor subunit. IL13 receptors are expressed on human B cells, basophils, eosinophils, mast cells, endothelial cells, fibroblasts, monocytes, macrophages, respiratory epithelial cells, and smooth muscle cells, but unlike IL4, not T cells. Thus IL13 does not appear to be important in the initial differentiation of CD4 T cells into Th2 cells, rather it is important in the effector phase of allergic inflammation (Hershey et al. 2003).

IL4 and IL13 induce "alternative activation" of macrophages, inducing an anti-inflammatory phenotype by signaling through IL4R alpha in a STAT6 dependent manner. This signaling plays an important role in the Th2 response, mediating anti-parasitic effects and aiding wound healing (Gordon & Martinez 2010, Loke et al. 2002)

There are two types of IL4 receptor complex (Andrews et al. 2006). Type I IL4R (IL4R1) is predominantly expressed on the surface of hematopoietic cells and consists of IL4R and IL2RG, the common gamma chain. Type II IL4R (IL4R2) is predominantly expressed on the surface of nonhematopoietic cells, it consists of IL4R and IL13RA1 and is also the type II receptor for IL13. (Obiri et al. 1995, Aman et al. 1996, Hilton et al. 1996, Miloux et al. 1997, Zhang et al. 1997). The second receptor for IL13 consists of IL4R and Interleukin-13 receptor alpha 2 (IL13RA2), sometimes called Interleukin-13 binding protein (IL13BP). It has a high affinity receptor for IL13 (Kd = 250 pmol/L) but is not sufficient to render cells responsive to IL13, even in the presence of IL4R (Donaldson et al. 1998). It is reported to exist in soluble form (Zhang et al. 1997) and when overexpressed reduces JAK-STAT signaling (Kawakami et al. 2001). It's function may be to prevent IL13 signalling via the functional IL4R:IL13RA1 receptor. IL13RA2 is overexpressed and enhances cell invasion in some human cancers (Joshi & Puri 2012).

The first step in the formation of IL4R1 (IL4:IL4R:IL2RB) is the binding of IL4 with IL4R (Hoffman et al. 1995, Shen et al. 1996, Hage et al. 1999). This is also the first step in formation of IL4R2 (IL4:IL4R:IL13RA1). After the initial binding of IL4 and IL4R, IL2RB binds (LaPorte et al. 2008), to form IL4R1. Alternatively, IL13RA1 binds, forming IL4R2. In contrast, the type II IL13 complex (IL13R2) forms with IL13 first binding to IL13RA1 followed by recruitment of IL4R (Wang et al. 2009).

Crystal structures of the IL4:IL4R:IL2RG, IL4:IL4R:IL13RA1 and IL13:IL4R:IL13RA1 complexes have been determined (LaPorte et al. 2008). Consistent with these structures, in monocytes IL4R is tyrosine phosphorylated in response to both IL4 and IL13 (Roy et al. 2002, Gordon & Martinez 2010) while IL13RA1 phosphorylation is induced only by IL13 (Roy et al. 2002, LaPorte et al. 2008) and IL2RG phosphorylation is induced only by IL4 (Roy et al. 2002).

Both IL4 receptor complexes signal through Jak/STAT cascades. IL4R is constitutively-associated with JAK2 (Roy et al. 2002) and associates with JAK1 following binding of IL4 (Yin et al. 1994) or IL13 (Roy et al. 2002). IL2RG constitutively associates with JAK3 (Boussiotis et al. 1994, Russell et al. 1994). IL13RA1 constitutively associates with TYK2 (Umeshita-Suyama et al. 2000, Roy et al. 2002, LaPorte et al. 2008, Bhattacharjee et al. 2013).

IL4 binding to IL4R1 leads to phosphorylation of JAK1 (but not JAK2) and STAT6 activation (Takeda et al. 1994, Ratthe et al. 2007, Bhattacharjee et al. 2013).

IL13 binding increases activating tyrosine-99 phosphorylation of IL13RA1 but not that of IL2RG. IL4 binding to IL2RG leads to its tyrosine phosphorylation (Roy et al. 2002). IL13 binding to IL4R2 leads to TYK2 and JAK2 (but not JAK1) phosphorylation (Roy & Cathcart 1998, Roy et al. 2002).

Phosphorylated TYK2 binds and phosphorylates STAT6 and possibly STAT1 (Bhattacharjee et al. 2013).

A second mechanism of signal transduction activated by IL4 and IL13 leads to the insulin receptor substrate (IRS) family (Kelly-Welch et al. 2003). IL4R1 associates with insulin receptor substrate 2 and activates the PI3K/Akt and Ras/MEK/Erk pathways involved in cell proliferation, survival and translational control. IL4R2 does not associate with insulin receptor substrate 2 and consequently the PI3K/Akt and Ras/MEK/Erk pathways are not activated (Busch-Dienstfertig & González-Rodríguez 2013).

References

Nelms K, Keegan AD, Zamorano J, Ryan JJ & Paul WE (1999). The IL-4 receptor: signaling mechanisms and biologic functions. Annu. Rev. Immunol., 17, 701-38. ↗

Hershey GK (2003). IL-13 receptors and signaling pathways: an evolving web. J. Allergy Clin. Immunol., 111, 677-90; quiz 691. ↗

Edit history

Date	Action	Author
2015-07-01	Authored	Jupe S
2015-07-01	Created	Jupe S
2016-09-02	Edited	Jupe S
2016-09-02	Reviewed	Leibovich SJ

Date	Action	Author
2019-03-13	Modified	Weiser D

Entities found in this pathway (15)

Input	UniProt Id	#FC
VCAM1	P19320	-3.60e+00
IL12A	P29459	-2.01e+00
LIF	P15018	-2.54e+00
HPS5	P0DJI8	1.59
CEBPD	P49716	1.48
FOXO1	Q12778	2.31
CDKN1A	P38936	-1.03e+00
FOXO3	O43524	1.26
PIK3R1	P27986	1.62
MAOA	P21397	3.28
SOCS1	O15524	-1.15e+00
HMOX1	P09601	-1.35e+00
S1PR1	P21453	-1.47e+00
MAOB	P21397	1.22
VEGFA	P15692	-1.23e+00

Input	Ensembl Id	#FC
VCAM1	ENSG00000162692	-3.60e+00
IL12A	ENSG00000168811	-2.01e+00
LIF	ENSG00000128342	-2.54e+00
CEBPD	ENSG00000221869	1.48
FOXO1	ENSG00000150907	2.31
CDKN1A	ENSG00000124762	-1.03e+00
FOXO3	ENSG00000118689	1.26
PIK3R1	ENSG00000145675	1.62
MAOA	ENSG00000189221	3.28
SOCS1	ENSG00000185338	-1.15e+00
HMOX1	ENSG00000100292	-1.35e+00
S1PR1	ENSG00000170989	-1.47e+00
VEGFA	ENSG00000112715	-1.23e+00

Interactors found in this pathway (3)

Input	UniProt Id	Interacts with	#FC
PIK3R1	P27986-2, P27986	P48023, O15524	1.62
THBS1	P07996-PRO_0000035842	P16671	1.94

Input	ChEBI Id	Interacts with	#FC
FAM20A	Q96MK3	15422	1.09

3. Laminin interactions ([R-HSA-3000157](R-HSA-3000157))
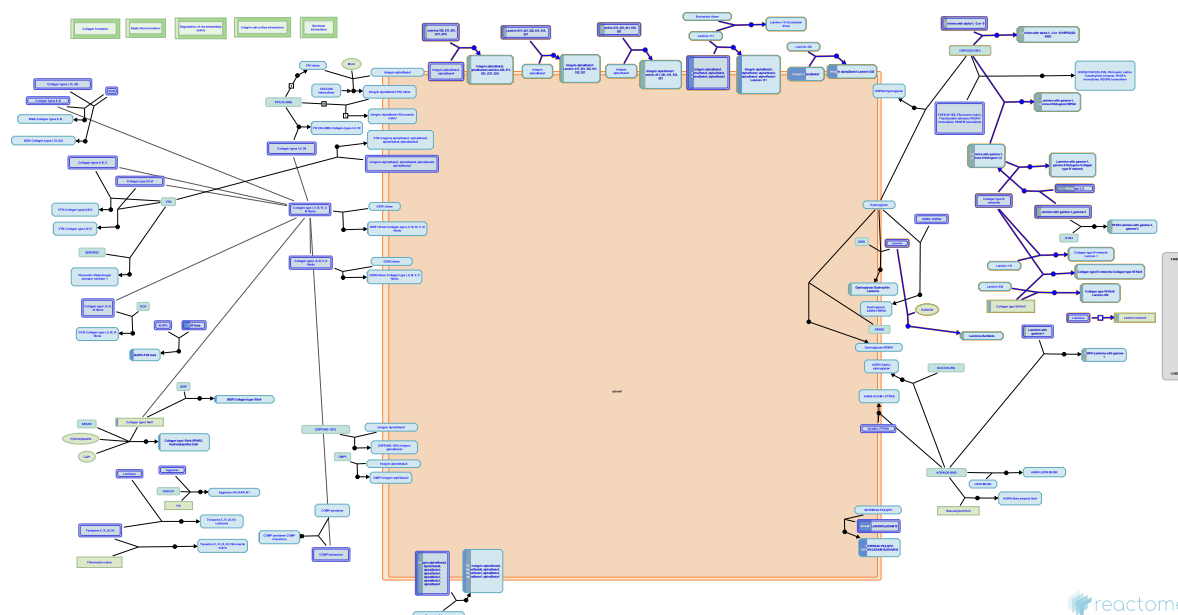
Laminins are a large family of conserved, multidomain trimeric basement membrane proteins. There are many theoretical trimer combinations but only 18 have been described (Domogatskaya et al. 2012, Miner 2008, Macdonald et al. 2010) and the existence of isoforms laminin-212 and/or laminin-222 (Durbeej et al. 2010) awaits further confirmation. The chains assemble through coiled-coil domains at their C-terminal end. Alpha chains additionally have a large C-terminal globular domain containing five LG subdomains (LG1-5). The N termini are often referred to as the short arms. These have varying numbers of laminin-type epidermal growth factor-like (LE) repeats. Trimer assembly is controlled by highly specific coiled-coil interactions (Domogatskaya et al. 2012). Some laminin isoforms are modified extracellularly by proteolytic processing at the N- or C-terminal ends prior to their binding to cellular receptors or other matrix molecules (Tzu & Marinkovitch 2008).

The cell adhesion properties of laminins are mediated primarily through the alpha chain G domain to integrins, dystroglycan, Lutheran glycoprotein, or sulfated glycolipids. The N-terminal globular domains of the alpha-1 (Colognato-Pyke et al. 1995) and alpha-2 chains (Colognato et al. 1997) and globular domains VI (Nielsen & Yamada 2001) and IVa (Sasaki & Timpl 2001) of the alpha-5 chain can bind to several integrin isoforms (alpha1beta1, alpha2beta1, alpha3beta1, and alphaVbeta3), which enables cell binding at both ends of laminins with these alpha chains.

References

Domogatskaya A, Rodin S & Tryggvason K (2012). Functional diversity of laminins. Annu. Rev. Cell Dev. Biol., 28, 523-53. ⤴

Edit history

Date	Action	Author
2008-05-07	Reviewed	Hynes R, Humphries MJ, Yamada KM
2012-08-08	Authored	Jupe S
2013-01-24	Created	Jupe S
2013-08-13	Edited	Jupe S

Date	Action	Author
2013-08-13	Reviewed	Ricard-Blum S
2019-03-08	Modified	Weiser D

Entities found in this pathway (6)

Input	UniProt Id	#FC
COL7A1	Q02388	1.22
COL4A4	P53420	2.02
COL4A1	P02462	1.33
LAMA2	P24043	2.07
ITGA2	P17301	-1.04e+00
NID1	P14543	1.54

4. Antagonism of Activin by Follistatin (R-HSA-2473224)
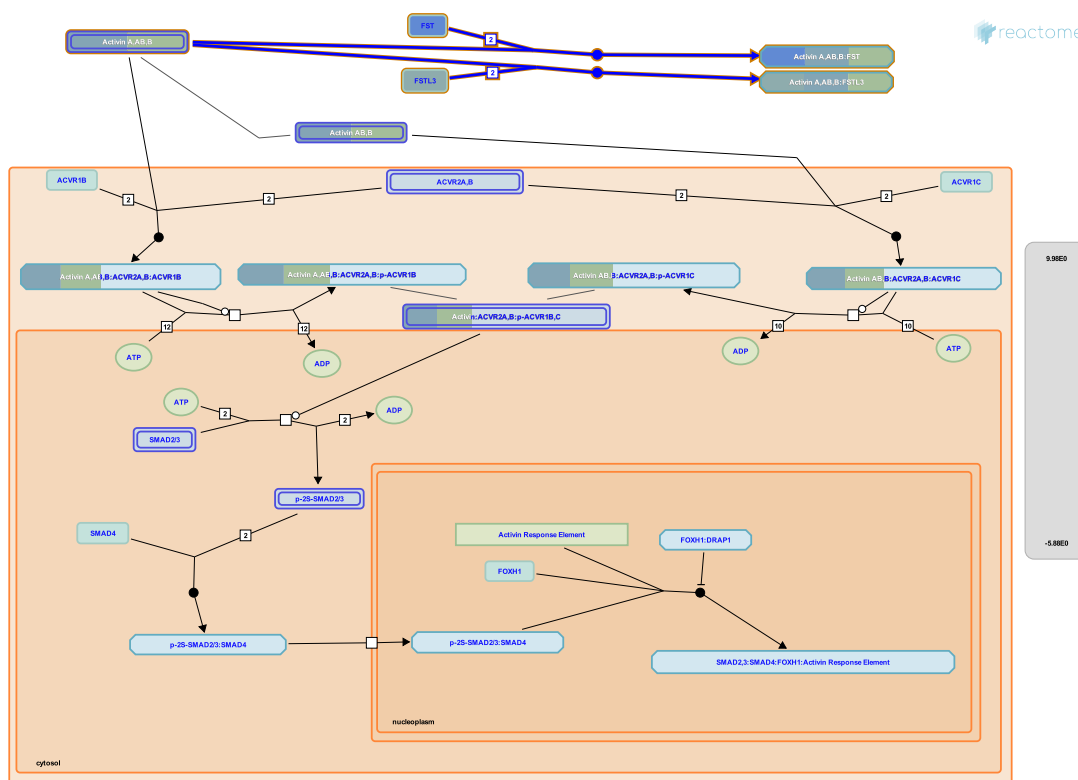
Cellular compartments: extracellular region.

Both Follistatin (FST) and Follistatin-like-3 (FSTL3) irreversibly bind Activin dimers and prevent Activin from interacting with its receptor (reviewed in Schneyer et al. 2004, Xia and Schneyer 2009). Though functionally similar in vitro, FST and FSTL3 do not function identically in vivo. Mice lacking FST die shortly after birth due to defects in muscle and bone (Matzuk et al. 1995); mice lacking FSTL3 are viable but have altered glucose metabolism (Mukherjee et al. 2007).

References

Schneyer A, Sidis Y, Xia Y, Saito S, del Re E, Lin HY & Keutmann H (2004). Differential actions of follistatin and follistatin-like 3. Mol. Cell. Endocrinol., 225, 25-8. ⤯

Xia Y & Schneyer AL (2009). The biology of activin: recent advances in structure, regulation and function. J. Endocrinol., 202, 1-12. ⤯

Matzuk MM, Lu N, Vogel H, Sellheyer K, Roop DR & Bradley A (1995). Multiple defects and perinatal death in mice deficient in follistatin. Nature, 374, 360-3. ⤯

Mukherjee A, Sidis Y, Mahan A, Raher MJ, Xia Y, Rosen ED, ... Schneyer AL (2007). FSTL3 deletion reveals roles for TGF-beta family ligands in glucose and fat homeostasis in adults. Proc. Natl. Acad. Sci. U.S.A., 104, 1348-53. ⤯

Edit history

Date	Action	Author
2012-09-21	Edited	May B
2012-09-21	Authored	May B

Date	Action	Author
2012-09-22	Created	May B
2012-11-14	Reviewed	Chen YG
2019-03-08	Modified	Weiser D

Entities found in this pathway (4)

Input	UniProt Id	#FC
INHBB	P09529	3.64
INHBA	P08476	1.07
FST	P19883	-1.78e+00
FSTL3	O95633	1.83

Interactors found in this pathway (2)

Input	UniProt Id	Interacts with	#FC
ADAM12	O43184-2	O95633	-1.84e+00
CREB5	Q02930-3	P19883	-1.98e+00

5.   Anchoring fibril formation (R-HSA-2214320)

Cellular compartments: extracellular region.

Collagen VII forms anchoring fibrils, composed of antiparallel dimers that connect the dermis to the epidermis (Bruckner-Tuderman 2009, Has & Kern 2010). During fibrillogenesis, the nascent type VII procollagen molecules dimerize in an antiparallel manner. The C-propeptide is then removed by Bone morphogenetic protein 1 (Rattenholl et al. 2002) and the processed antiparallel dimers laterally aggregate (Villone et al. 2008, Gordon & Hahn 2010).

References

Chung HJ & Uitto J (2010). Type VII collagen: the anchoring fibril protein at fault in dystrophic epidermolysis bullosa. Dermatol Clin, 28, 93-105. 🔗

Edit history

Date	Action	Author
2012-04-30	Authored	Jupe S
2012-04-30	Created	Jupe S
2012-10-08	Reviewed	Kalamajski S, Raleigh S
2012-11-12	Edited	Jupe S
2012-11-19	Reviewed	Ricard-Blum S
2019-03-08	Modified	Weiser D

Entities found in this pathway (4)

Input	UniProt Id	#FC
COL7A1	Q02388	1.22
COL4A4	P53420	2.02

Input	UniProt Id	#FC
COL4A1	P02462	1.33
COL1A1	P02452	-1.31e+00

6.   Defective B3GALTL causes Peters-plus syndrome (PpS) (R-HSA-5083635)
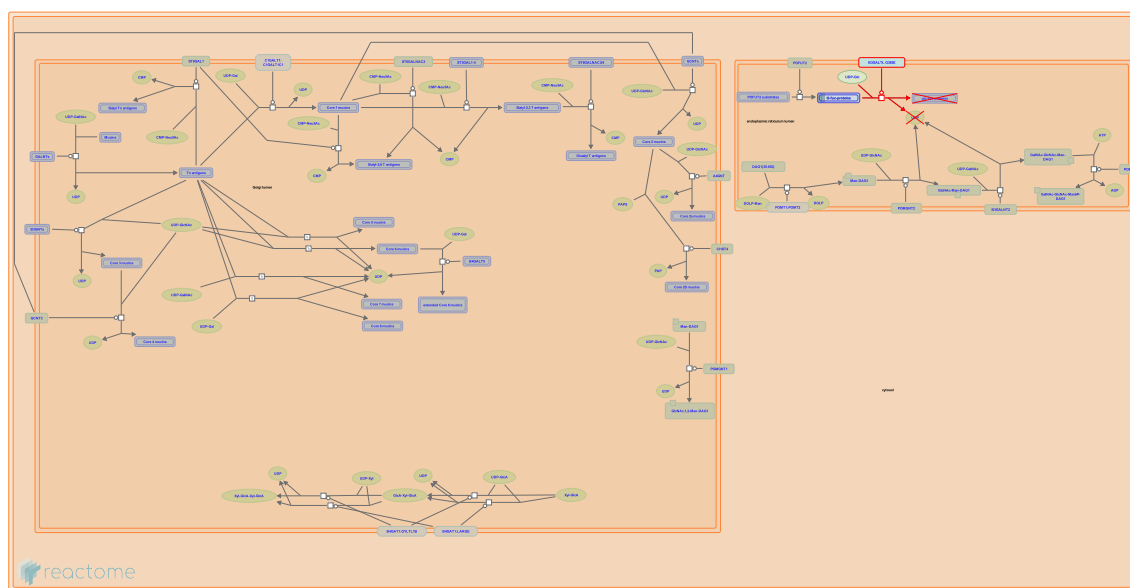
Diseases: eye disease, orofacial cleft.

Human beta-1,3-glucosyltransferase like protein (B3GALTL, HGNC Approved Gene Symbol: B3GLCT; MIM:610308; CAZy family GT31), localised on the ER membrane, glucosylates O-fucosylated proteins. The resultant glc-beta-1,3-fuc disaccharide modification on thrombospondin type 1 repeat (TSR1) domain-containing proteins is thought to assist in the secretion of many of these proteins from the ER lumen, and mediate an ER quality-control mechanism of folded TSRs (Vasudevan et al. 2015). Defects in B3GALTL can cause Peters plus syndrome (PpS; MIM:261540), an autosomal recessive disorder characterised by anterior eye chamber defects, short stature, delay in growth and mental developmental and cleft lip and/or palate (Heinonen & Maki 2009).

References

Heinonen TY & Maki M (2009). Peters'-plus syndrome is a congenital disorder of glycosylation caused by a defect in the beta1,3-glucosyltransferase that modifies thrombospondin type 1 repeats. Ann. Med., 41, 2-10.

Vasudevan D, Takeuchi H, Johar SS, Majerus E & Haltiwanger RS (2015). Peters plus syndrome mutations disrupt a noncanonical ER quality-control mechanism. Curr. Biol., 25, 286-95.

Edit history

Date	Action	Author
2013-11-07	Edited	Jassal B
2013-11-07	Authored	Jassal B
2013-11-07	Created	Jassal B
2015-12-18	Modified	Jassal B
2015-12-18	Reviewed	Hansen L, Joshi HJ

Entities found in this pathway (6)

Input	UniProt Id	#FC
ADAMTS1	Q9UHI8	2.28
ADAMTS14	Q8WXS8	-2.42e+00
ADAMTSL1	Q8N6G6	-1.05e+00
ADAMTS5	Q9UNA0	2.12
SPON1	Q9HCB6	1.8
THBS1	P07996	1.94

7. Metallothioneins bind metals ([R-HSA-5661231](#))
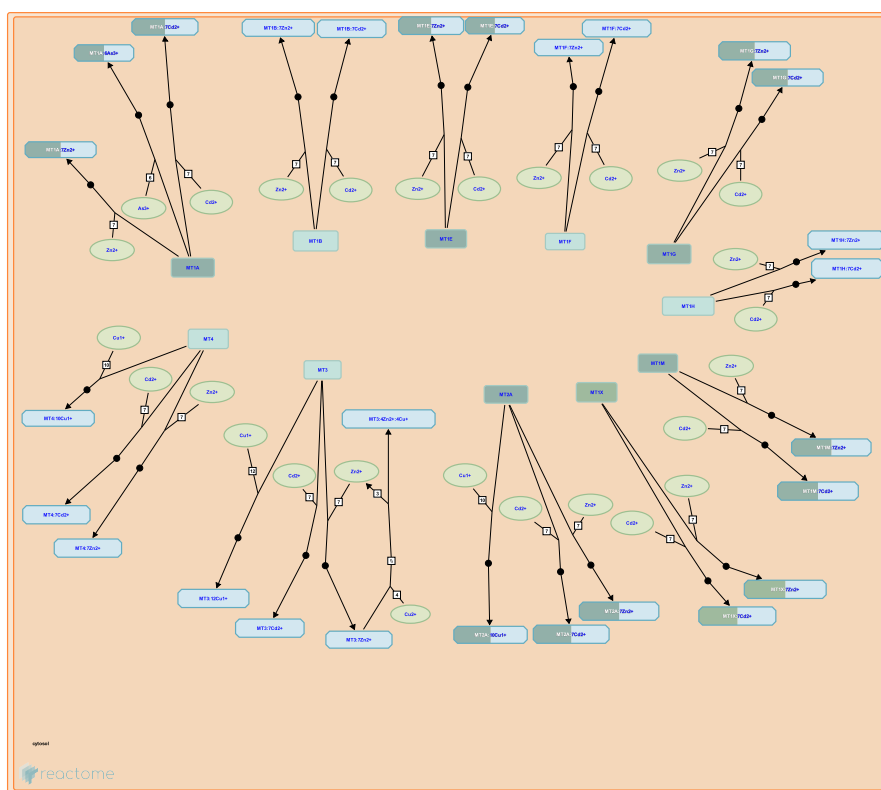
Metallothioneins are highly conserved, cysteine-rich proteins that bind metals via thiolate bonds (recent general reviews in Capdevila et al. 2012, Blindauer et al. 2014, reviews of mammalian metallothioneins in Miles et al. 2000, Maret 2011, Vasak and Meloni 2011, Thirumoorthy et al. 2001, Babula et al. 2012). Mammals contain 4 general metallothionein isoforms (MT1,2,3,4). The MT1 isoform has radiated in primates to 8 or 9 functional proteins (depending on classification of MT1L). Each mammalian metallothionein binds a total of 7 divalent metal ions in two clusters, the alpha and beta clusters. Though the functions of metallothioneins have not been fully elucidated, they appear to participate in detoxifying heavy metals (reviewed in Sharma et al. 2013), storing and transporting zinc, and redox biochemistry. Metallothioneins interact with many other cellular proteins, with most interactions involving proteins of the central nervous system (reviewed in Atrian and Capdevila 2013).

References

Miles AT, Hawksworth GM, Beattie JH & Rodilla V (2000). Induction, regulation, degradation, and biological significance of mammalian metallothioneins. Crit. Rev. Biochem. Mol. Biol., 35, 35-70 . ↗

Babula P, Masarik M, Adam V, Eckschlager T, Stiborova M, Trnkova L, ... Kizek R (2012). Mammalian metallothioneins: properties and functions. Metallomics, 4, 739-50. ↗

Vašák M & Meloni G (2011). Chemistry and biology of mammalian metallothioneins. J. Biol. Inorg. Chem., 16, 1067-78. ↗

Thirumoorthy N, Shyam Sunder A, Manisenthil Kumar K, Senthil Kumar M, Ganesh G & Chatterjee M (2011). A review of metallothionein isoforms and their role in pathophysiology. World J Surg Oncol, 9, 54. ↗

Maret W (2011). Redox biochemistry of mammalian metallothioneins. J. Biol. Inorg. Chem., 16, 1079-86. 🔗

Edit history

Date	Action	Author
2015-01-07	Edited	May B
2015-01-07	Authored	May B
2015-01-10	Created	May B
2015-09-19	Reviewed	Atrian S
2019-03-08	Modified	Weiser D

Entities found in this pathway (4)

Input	UniProt Id	#FC
MT1X	P80297	3.24
MT1M	P13640, Q8N339	2.4
MT2A	P02795, P04731	2.19
MT1E	P04732	2.16

8. O-glycosylation of TSR domain-containing proteins (R-HSA-5173214)
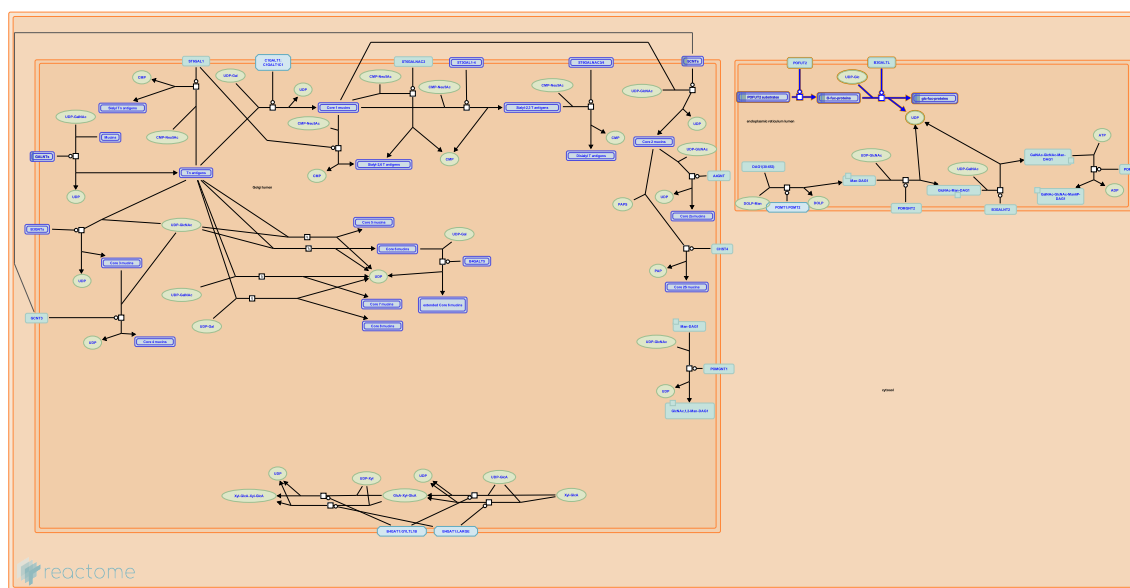
The O-fucosylation of proteins containing thrombospondin type 1 repeat (TSR) domains is an important PTM, regulating many biological processes such as Notch signalling, inflammation, wound healing, angiogenesis amd neoplasia (Adams & Tucker 2000, Moremen et al. 2012). Fucose addition is carried out by two protein fucosyltransferases, POFUT1 and 2. Only POFUT2 recognises the consensus sequence CSXS/TCG found in TSR1 domains and the fucosyl residue is attached to the hydroxyl group of conserved serine (S) or threonine (T) residues within the consensus sequence. The modification was first demonstrated on thrombospondin 1, found in platelets and the ECM (Hofsteenge et al. 2001, Luo et al. 2006). The resulting O-fucosyl-protein is subsequently a substrate for beta-1,3-glucosyltransferase-like protein (B3GALTL), which adds a glucosyl moiety to form the rare disaccharide modification Glc-beta-1,3-Fuc. More than 60 human proteins contain TSR1 domains, The disaccharide modification has been demonstrated on a small number of these TSR1 domain-containing proteins such as thrombospondin 1 (Hofsteenge et al. 2001, Luo et al. 2006), properdin (Gonzalez de Peredo et al. 2002) and F-spondin (Gonzalez de Peredo et al. 2002). The ADAMTS (a disintegrin-like and metalloprotease domain with thrombospondin type-1 repeats) superfamily consists of 19 secreted metalloproteases (ADAMTS proteases) and at lease five ADAMTS-like proteins in humans. Five members of the ADAMTS superfamily have also had experimental confirmation of the disaccharide modification. Examples are ADAMTS13 (Ricketts et al. 2007) and ADAMTSL1 (Wang et al. 2007). In the two reactions described here, the TSR1 domain-containing proteins with similarity to the experimentally confirmed ones are included as putative substrates.

References

Adams JC & Tucker RP (2000). The thrombospondin type 1 repeat (TSR) superfamily: diverse proteins with related roles in neuronal development. Dev. Dyn., 218, 280-99. ⧉

Moremen KW, Tiemeyer M & Nairn AV (2012). Vertebrate protein glycosylation: diversity, synthesis and function. Nat. Rev. Mol. Cell Biol., 13, 448-62. ⧉

Hofsteenge J, Huwiler KG, Macek B, Hess D, Lawler J, Mosher DF & Peter-Katalinic J (2001). C-mannosylation and O-fucosylation of the thrombospondin type 1 module. J. Biol. Chem., 276, 6485-98. ⧉

Luo Y, Nita-Lazar A & Haltiwanger RS (2006). Two distinct pathways for O-fucosylation of epidermal growth factor-like or thrombospondin type 1 repeats. J. Biol. Chem., 281, 9385-92. ⎘

Ricketts LM, Dlugosz M, Luther KB, Haltiwanger RS & Majerus EM (2007). O-fucosylation is required for ADAMTS13 secretion. J. Biol. Chem., 282, 17014-23. ⎘

Edit history

Date	Action	Author
2013-11-25	Edited	Jassal B
2013-11-25	Authored	Jassal B
2013-11-25	Created	Jassal B
2014-02-07	Reviewed	D'Eustachio P
2019-03-08	Modified	Weiser D

Entities found in this pathway (6)

Input	UniProt Id	#FC
ADAMTS1	Q9UHI8	2.28
ADAMTS14	Q8WXS8	-2.42e+00
ADAMTSL1	Q8N6G6	-1.05e+00
ADAMTS5	Q9UNA0	2.12
SPON1	Q9HCB6	1.8
THBS1	P07996	1.94

9. Collagen chain trimerization (R-HSA-8948216)
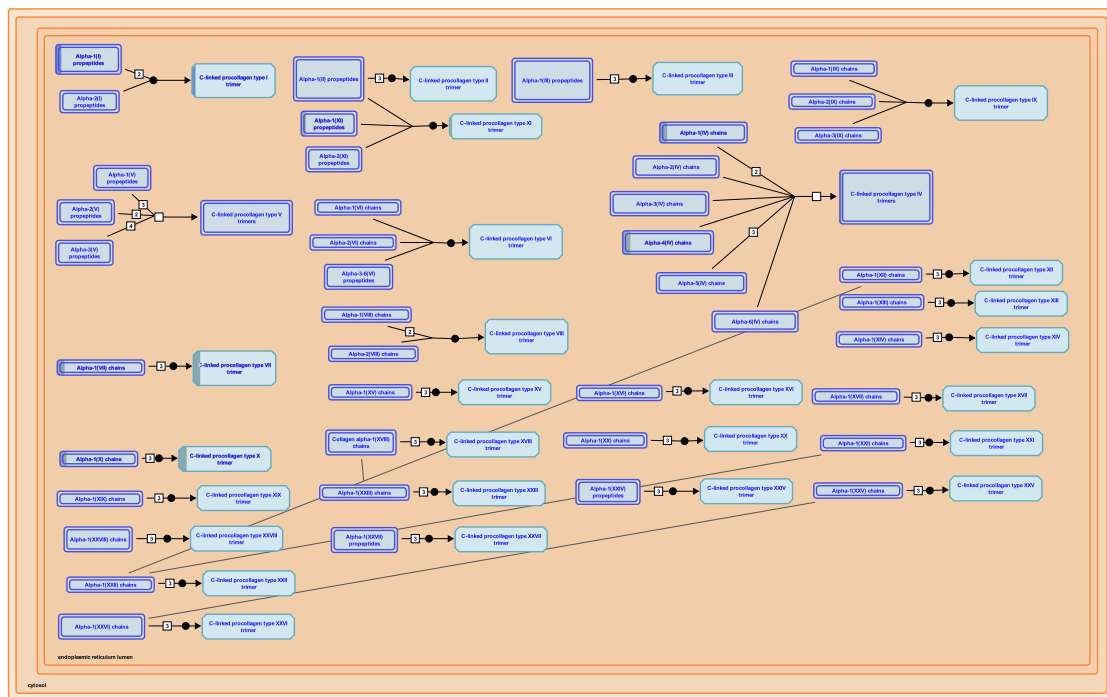
The C-propeptides of collagen propeptide chains are essential for the association of three peptide chains into a trimeric but non-helical procollagen. This initial binding event determines the composition of the trimer, brings the individual chains into the correct register and initiates formation of the triple helix at the C-terminus, which then proceeds towards the N-terminus in a zipper-like fashion (Engel & Prockop 1991). Most early refolding studies were performed with collagen type III, which contains a disulfide linkage at the C-terminus of its triple helix (Bächinger et al. 1978, Bruckner et al. 1978) that acts as a permanent linker even after removal of the non-collagenous domains.

Mutations within the C-propeptides further suggest that they are crucial for the correct interaction of the three polypeptide chains and for subsequent correct folding (refs. in Boudko et al. 2011).

References

Byers PH, Click EM, Harper E & Bornstein P (1975). Interchain disulfide bonds in procollagen are located in a large nontriple-helical COOH-terminal domain. Proc Natl Acad Sci U S A, 72, 3009-13.

Bächinger HP, Brückner P, Timpl R & Engel J (1978). The role of cis-trans isomerization of peptide bonds in the coil leads to and comes from triple helix conversion of collagen. Eur J Biochem, 90, 605-13.
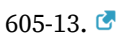
Edit history

Date	Action	Author
2012-04-11	Authored	Jupe S
2012-05-24	Reviewed	Canty-Laird EG
2016-11-03	Edited	Jupe S
2016-11-11	Created	Jupe S

Date	Action	Author
2019-03-08	Modified	Weiser D

Entities found in this pathway (5)

Input	UniProt Id	#FC
COL7A1	Q02388	1.22
COL4A4	P53420	2.02
COL4A1	P02462, Q03692	1.33
COL11A1	P12107	2.36
COL1A1	P02452	-1.31e+00

10.   Response to metal ions (R-HSA-5660526)
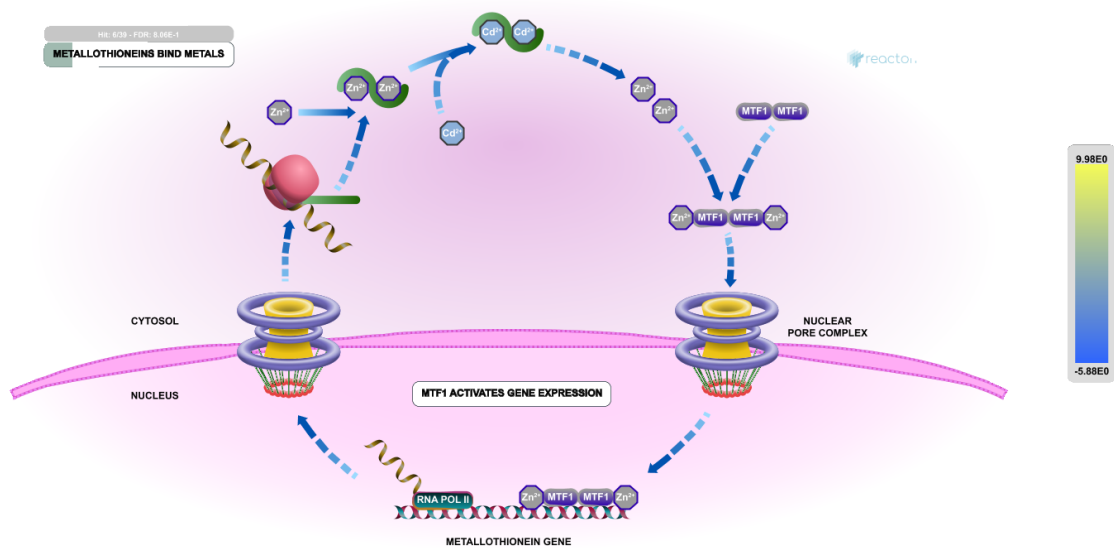
Though metals such as zinc, copper, and iron are required as cofactors for cellular enzymes they can also catalyze damaging metal substitution or unspecific redox reactions if they are not sequestered. The transcription factor MTF1 directs the major cellular response to zinc, cadmium, and copper. MTF1 activates gene expression to up-regulate genes encoding proteins, such as metallothioneins and glutamate-cysteine ligase (GCLC), involved in sequestering metals. MTF1 represses gene expression to down-regulate genes encoding transporters that import the metals into the cell (reviewed in Laity and Andrews 2007, Jackson et al. 2008, Günther et al. 2012, Dong et al. 2015). During activation MTF1 in the cytosol binds zinc ions and is translocated into the nucleus, where it binds metal response elements in the promoters of target genes. Activation of MTF1 by cadmium and copper appears to be indirect as these metals displace zinc from metallothioneins and the displaced zinc then binds MTF1.

Metallothioneins bind metals and participate in detoxifying heavy metals, storing and transporting zinc, and redox biochemistry.

References

Dong G, Chen H, Qi M, Dou Y & Wang Q (2015). Balance between metallothionein and metal response element binding transcription factor 1 is mediated by zinc ions (review). Mol Med Rep, 11, 1582-6. 🔗

Günther V, Lindert U & Schaffner W (2012). The taste of heavy metals: gene regulation by MTF-1. Biochim. Biophys. Acta, 1823, 1416-25. 🔗

Jackson KA, Valentine RA, Coneyworth LJ, Mathers JC & Ford D (2008). Mechanisms of mammalian zinc-regulated gene expression. Biochem. Soc. Trans., 36, 1262-6. 🔗

Laity JH & Andrews GK (2007). Understanding the mechanisms of zinc-sensing by metal-response element binding transcription factor-1 (MTF-1). Arch. Biochem. Biophys., 463, 201-10. 🔗

Edit history

Date	Action	Author
2014-12-28	Edited	May B
2014-12-28	Authored	May B
2015-01-05	Created	May B
2015-09-19	Reviewed	Atrian S
2019-03-08	Modified	Weiser D

Entities found in this pathway (4)

Input	UniProt Id	#FC
MT1X	P80297	3.24
MT1M	P13640, Q8N339	2.4
MT2A	P02795, P04731	2.19
MT1E	P04732	2.16

11. Regulation of FZD by ubiquitination ([R-HSA-4641263](R-HSA-4641263))
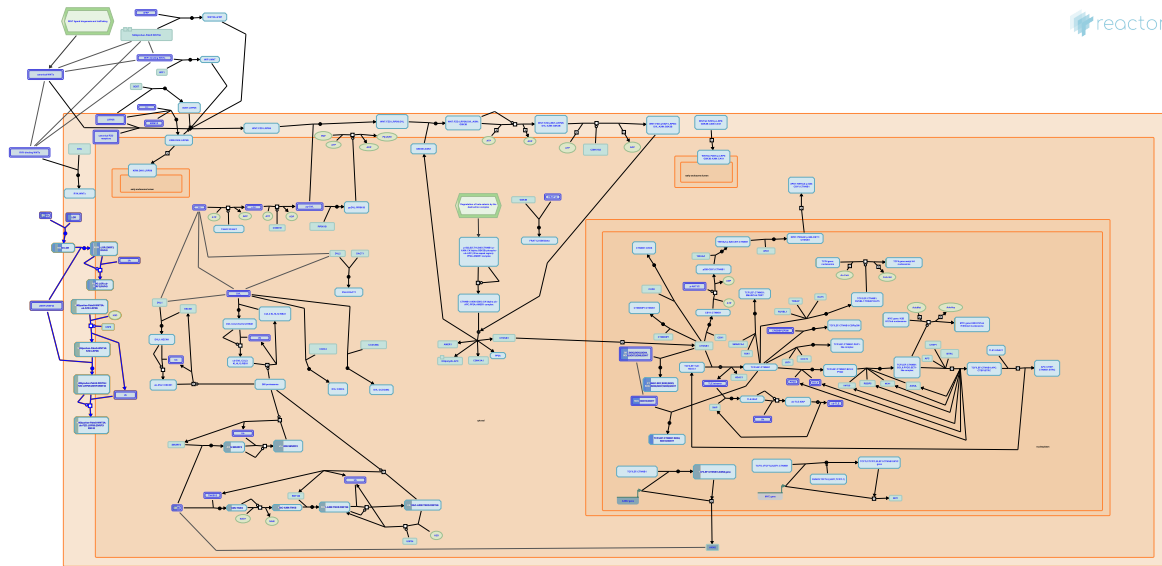
WNT responsiveness is influenced by expression levels of FZD and LRP proteins. Levels of these receptors at the cell surface are regulated in part by endocytosis, but the mechanisms are not fully elucidated (Garliardi et al, 2008). A number of recent studies have identified a role for ubiquitination in the localization and turnover of WNT receptors at the plasma membrane. ZNRF3 and RNF43 are E3 ligases that have been shown to ubiquitinate FZD proteins and promote their lysosomal degradation, while the deubiquitinating enzyme USP8 promotes recycling of the receptor back to the plasma membrane (Hao et al, 2012; Mukai et al, 2010). This balance of ubiquitination and deubiquitination is in turn regulated by the R-spondin (RSPO) proteins, agonists of WNT signaling which appear to act by downregulating ZNRF3 and RNF43, thus potentiating both canonical and non-canonical pathways (Hao et al, 2012; reviewed in Abo and Clevers, 2012; Fearon and Spence, 2012, Papartriantafyllou, 2012).

References

Hao HX, Xie Y, Zhang Y, Charlat O, Oster E, Avello M, ... Cong F (2012). ZNRF3 promotes Wnt receptor turnover in an R-spondin-sensitive manner. Nature, 485, 195-200.

Mukai A, Yamamoto-Hino M, Awano W, Watanabe W, Komada M & Goto S (2010). Balanced ubiquitylation and deubiquitylation of Frizzled regulate cellular responsiveness to Wg/Wnt. EMBO J., 29, 2114-25.

Gagliardi M, Piddini E & Vincent JP (2008). Endocytosis: a positive or a negative influence on Wnt signalling?. Traffic, 9, 1-9.

Abo A & Clevers HC (2012). Modulating WNT receptor turnover for tissue repair. Nat. Biotechnol., 30, 835-6.

Fearon ER & Spence JR (2012). Cancer biology: a new RING to Wnt signaling. Curr. Biol., 22, R849-51.

Edit history

Date	Action	Author
2007-09-04	Edited	Matthews L
2013-09-24	Authored	Rothfels K

Date	Action	Author
2013-09-28	Created	Rothfels K
2013-10-03	Edited	Gillespie ME
2014-01-22	Reviewed	Rajakulendran N
2014-02-15	Reviewed	van Amerongen R
2014-04-22	Reviewed	Kikuchi A
2019-03-08	Modified	Weiser D

Entities found in this pathway (4)

Input	UniProt Id	#FC
LGR4	Q9BXB1	-1.10e+00
FZD8	Q9H461	2.44
RSPO2	Q2I0M5, Q6UXX9	-1.48e+00
RSPO1	Q2MKA7	1.33

12. Microtubule-dependent trafficking of connexons from Golgi to the plasma membrane (R-HSA-190840)
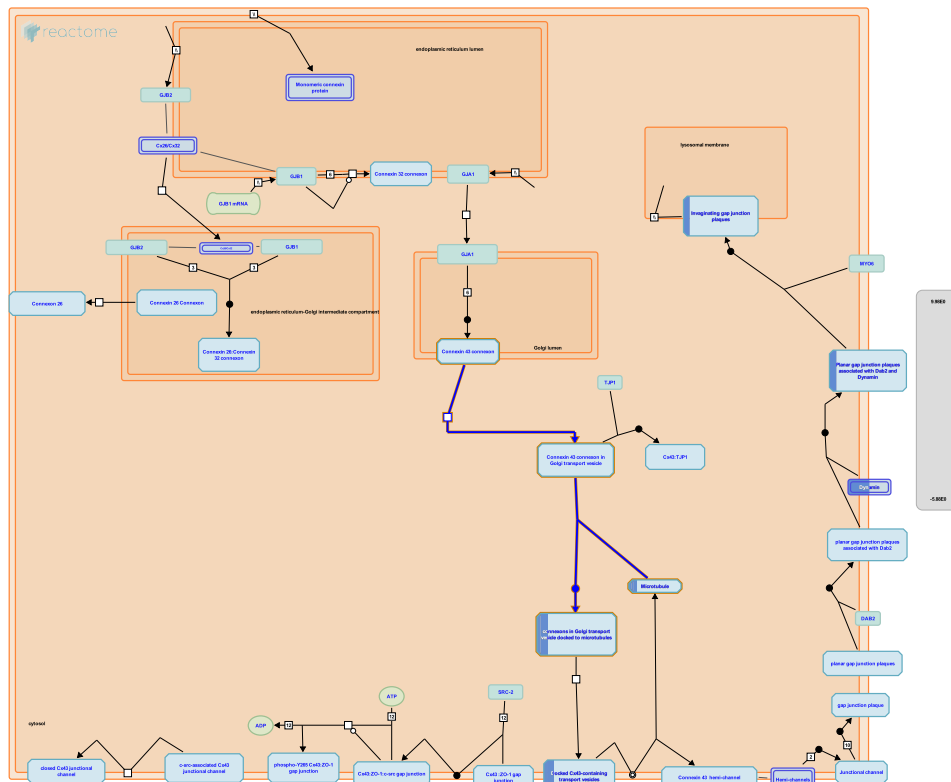
Cellular compartments: cytosol.

Through videomicroscopy, a saltatory transport of connexon vesicles along curvilinear microtubules from the Golgi to the plasma membrane has been observed (Lauf et al., 2002). Such a transport system has been described for similar secretory vesicles (Toomre et al., 1999).

References

Lauf U, Giepmans BN, Lopez P, Braconnot S, Chen SC & Falk MM (2002). Dynamic trafficking and delivery of connexons to the plasma membrane and accretion to gap junctions in living cells. Proc Natl Acad Sci U S A, 99, 10446-51.

Edit history

Date	Action	Author
2007-01-03	Authored	Gilleron J, Segretain D, Falk MM
2007-01-09	Created	Matthews L
2007-04-12	Edited	Matthews L
2019-03-08	Modified	Weiser D

Entities found in this pathway (3)

Input	UniProt Id	#FC
TUBA4A	P68363, P68366	-1.45e+00
TUBB3	Q13509	-1.49e+00
TUBA1A	P68363, Q71U36	-1.29e+00

13. Transport of connexons to the plasma membrane (R-HSA-190872)
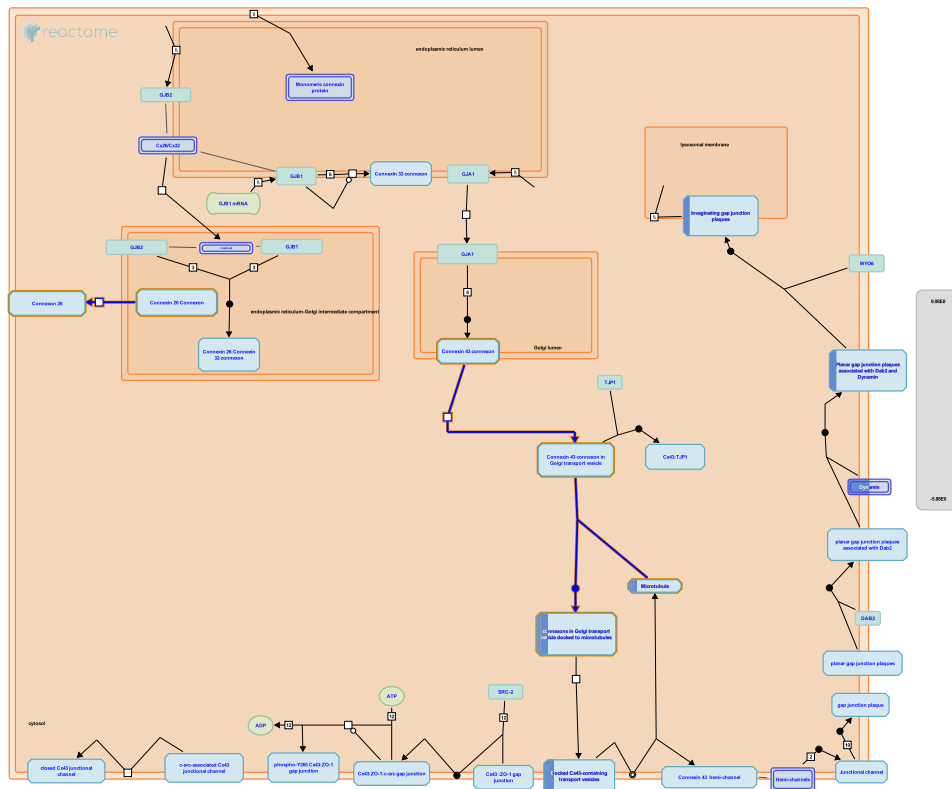
Cellular compartments: cytosol.

Following connexon oligomerization, the hemichannels must be transported to the plasma membrane. This has been shown to occur in transport vesicles called "cargo containers". Most of post-Golgi cargo containers have a diameter of of 50- 200 nm (Lauf et al., 2002). Recently direct transport of connexins to GJ assembly sides has been described (Shaw et al., 2007). Besides microtuble-dependent trafficking, a microtubule-independent delivery pathway may exist as concluded from studies using the secretory transport inhibitor, Brefeldin A (Musil and Goodenough 1993; De Sousa et al. 1993; Laird et al. 1995).

References

De Sousa PA, Valdimarsson G, Nicholson BJ & Kidder GM (1993). Connexin trafficking and the control of gap junction assembly in mouse preimplantation embryos. Development, 117, 1355-67. ↪

Lauf U, Giepmans BN, Lopez P, Braconnot S, Chen SC & Falk MM (2002). Dynamic trafficking and delivery of connexons to the plasma membrane and accretion to gap junctions in living cells. Proc Natl Acad Sci U S A, 99, 10446-51. ↪

Laird DW, Castillo M & Kasprzak L (1995). Gap junction turnover, intracellular trafficking, and phosphorylation of connexin43 in brefeldin A-treated rat mammary tumor cells. J Cell Biol, 131, 1193-203. ↪

Shaw RM, Fay AJ, Puthenveedu MA, von Zastrow M, Jan YN & Jan LY (2007). Microtubule plus-end-tracking proteins target gap junctions directly from the cell interior to adherens junctions. Cell, 128, 547-60. ↪

Musil LS & Goodenough DA (1993). Multisubunit assembly of an integral plasma membrane channel protein, gap junction connexin43, occurs after exit from the ER. Cell, 74, 1065-77. ↪

Edit history

Date	Action	Author
2007-01-03	Authored	Gilleron J, Segretain D, Falk MM
2007-01-09	Created	Matthews L
2007-04-12	Edited	Matthews L
2019-03-08	Modified	Weiser D

Entities found in this pathway (3)

Input	UniProt Id	#FC
TUBA4A	P68363, P68366	-1.45e+00
TUBB3	Q13509	-1.49e+00
TUBA1A	P68363, Q71U36	-1.29e+00

14. Collagen degradation (R-HSA-1442490)

Collagen fibril diameter and spatial organisation are dependent on the species, tissue type and stage of development (Parry 1988). The lengths of collagen fibrils in mature tissues are largely unknown but in tendon can be measured in millimetres (Craig et al. 1989). Collagen fibrils isolated from adult bovine corneal stroma had ~350 collagen molecules in transverse section, tapering down to three molecules at the growing tip (Holmes & Kadler 2005).

The classical view of collagenases is that they actively unwind the triple helical chain, a process termed molecular tectonics (Overall 2002, Bode & Maskos 2003), before preferentially cleaving the alpha2 chain followed by the remaining chains (Chung et al. 2004). More recently it has been suggested that collagen fibrils exist in an equilibrium between protected and vulnerable states (Stultz 2002, Nerenberg & Stultz 2008). The prototypical triple-helical structure of collagen does not fit into the active site of collagenase MMPs. In addition the scissile bonds are not solvent-exposed and are therefore inaccessible to the collagenase active site (Chung et al. 2004, Stultz 2002). It was realized that collagen must locally unfold into non-triple helical regions to allow collagenolysis. Observations using circular dichroism and differential scanning calorimetry confirm that there is considerable heterogeneity along collagen fibres (Makareeva et al. 2008) allowing access for MMPs at physiological temperatures (Salsas-Escat et al. 2010).

Collagen fibrils with cut chains are unstable and accessible to proteinases that cannot cleave intact collagen strands (Woessner & Nagase 2000, Somerville et al. 2003). Continued degradation leads to the formation of gelatin (Lovejoy et al. 1999). Degradation of collagen types other than I-III is less well characterized but believed to occur in a similar manner.

Metalloproteinases (MMPs) play a major part in the degradation of several extracellular macromolecules including collagens. MMP1 (Welgus et al. 1981), MMP8 (Hasty et al. 1987), and MMP13 (Knauper et al. 1996), sometimes referred to as collagenases I, II and III respectively, are able to initiate the intrahelical cleavage of the major fibril forming collagens I, II and III at neutral pH, and thus thought to define the rate-limiting step in normal tissue remodeling events. All can cleave additional substrates including other collagen subtypes. Collagenases cut collagen alpha chains at a single conserved Gly-Ile/Leu site approximately 3/4 of the molecule's length from the N-terminus (Fields 1991, Chung et al. 2004). The cleavage site is characterised by the motif G(I/L)(A/L); the G-I/L bond is cleaved. In collagen type I this corresponds to G953-I954 in the Uniprot canonical alpha chain sequences (often given as G775-I776 in literature). It is not clear why only this bond is cleaved, as the motif occurs at several other places in the chain. MMP14, a membrane-associated MMP also known as Membrane-type matrix metalloproteinase 1 (MT-MMP1), is able to cleave collagen types I, II and III (Ohuchi et al. 1997).

References

Hadler-Olsen E, Fadnes B, Sylte I, Uhlin-Hansen L & Winberg JO (2011). Regulation of matrix metalloproteinase activity in health and disease. FEBS J, 278, 28-45. ⧉

Steinhusen U, Weiske J, Badock V, Tauber R, Bommert K & Huber O (2001). Cleavage and shedding of E-cadherin after induction of apoptosis. J. Biol. Chem., 276, 4972-80. ⧉

Shapiro SD (1998). Matrix metalloproteinase degradation of extracellular matrix: biological consequences. Curr Opin Cell Biol, 10, 602-8. ⧉

Edit history

Date	Action	Author
2011-07-12	Authored	Jupe S
2011-07-12	Created	Jupe S
2012-10-08	Reviewed	Sorsa T
2012-11-12	Edited	Jupe S
2019-03-08	Modified	Weiser D

Entities found in this pathway (6)

Input	UniProt Id	#FC
MMP15	P51511	1.28
COL7A1	Q02388	1.22
COL4A4	P53420	2.02
COL4A1	P02462, Q03692	1.33
COL11A1	P12107	2.36
COL1A1	P02452	-1.31e+00

15. FOXO-mediated transcription of oxidative stress, metabolic and neuronal genes (R-HSA-9615017)
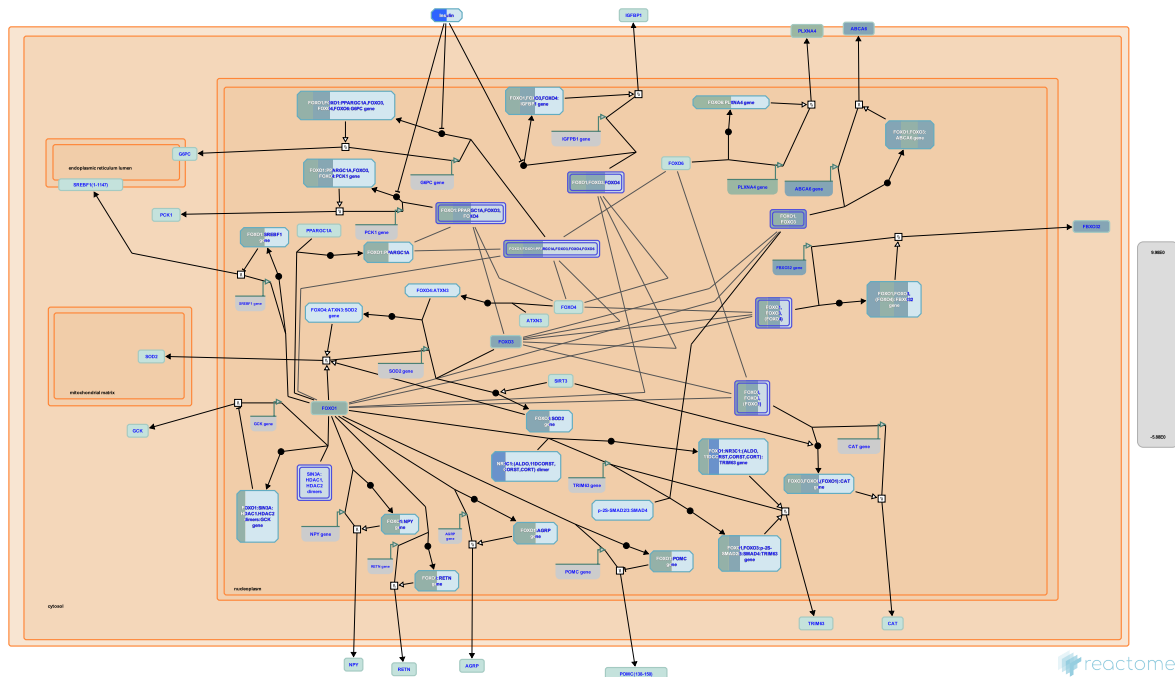
FOXO6, the least studied member of the FOXO family, directly stimulates transcription of PLXNA4 gene, encoding a co-factor for the semaphorin SEMA3A receptor. FOXO6-mediated regulation of PLXNA4 expression plays an important role in radial glia migration during cortical development (Paap et al. 2016).

FOXO-mediated up-regulation of genes involved in reduction of the oxidative stress burden is not specific to neurons, but plays an important role in neuronal survival and neurodegenerative diseases. FOXO3 and FOXO4, and possibly FOXO1, directly stimulate transcription of the SOD2 gene, encoding mitochondrial manganese-dependent superoxide dismutase, which converts superoxide to the less harmful hydrogen peroxide and oxygen (Kops et al. 2002, Hori et al. 2013, Araujo et al. 2011, Guan et al. 2016). FOXO4 stimulates SOD2 gene transcription in collaboration with ATXN3, a protein involved in spinocerebellar ataxia type 3 (SCA3) (Araujo et al. 2011). FOXO3 and FOXO6, and possibly FOXO1, directly stimulate transcription of the CAT gene, encoding catalase, an enzyme that converts hydrogen peroxide to water and oxygen, thus protecting cells from the oxidative stress (Awad et al. 2014, Kim et al. 2014, Rangarajan et al. 2015, Song et al. 2016, Liao et al. 2016, Guo et al. 2016).

FOXO transcription factors regulate transcription of several genes whose protein products are secreted from hypothalamic neurons to control appetite and food intake: NPY gene, AGRP gene and POMC gene. At low insulin levels, characteristic of starvation, FOXO transcription factors bind to insulin responsive elements (IRES) in the regulatory regions of NPY, AGRP and POMC gene. FOXO1 directly stimulates transcription of the NPY gene, encoding neuropeptide-Y (Kim et al. 2006, Hong et al. 2012), and the AGRP gene, encoding Agouti-related protein (Kitamura et al. 2006, Kim et al. 2006), which both stimulate food intake. At the same time, FOXO1 directly represses transcription of the POMC gene, encoding melanocyte stimulating hormone alpha , which suppresses food intake (Kitamura et al. 2006, Kim et al. 2006). When, upon food intake, blood insulin levels rise, insulin-mediated activation of PI3K/AKT signaling inhibits FOXO transcriptional activity.

In liver cells, FOXO transcription factors regulate transcription of genes involved in gluconeogenesis: G6PC gene, encoding glucose-6-phosphatase and PCK1 gene, encoding phosphoenolpyruvate carboxykinase. Actions of G6PC and PCK1 enable steady glucose blood levels during fasting. FOXO1, FOXO3 and FOXO4 directly stimulate PCK1 gene transcription (Hall et al. 2000, Yang et al. 2002, Puigserver et al. 2003), while all four FOXOs, FOXO1, FOXO3, FOXO4 and FOXO6 directly stimulate G6PC gene transcription (Yang et al. 2002, Puigserver et al. 2003, Onuma et al. 2006, Kim et al. 2011). FOXO-mediated induction of G6PC and PCK1 genes is negatively regulated by insulin-induced PI3K/AKT signaling.

FOXO1, FOXO3 and FOXO4 directly stimulate transcription of the IGFBP1 gene, encoding insulin growth factor binding protein 2 (Tang et al. 1999, Kops et al. 1999, Hall et al. 2000, Yang et al. 2002), which increases sensitivity of cells to insulin.

FOXO1 and FOXO3 directly stimulate transcription of the ABCA6 (ATP-binding cassette sub-family A member 6) gene, encoding a putative transporter protein that is thought to be involved in lipid homeostasis (Gai et al. 2013). The GCK (glucokinase) gene is another gene involved in lipid homeostasis that is regulated by FOXOs. FOXO1, acting with the SIN3A:HDAC complex, directly represses the GCK gene transcription, thus repressing lipogenesis in the absence of insulin (Langlet et al. 2017). The SREBF1 (SREBP1) gene, which encodes a transcriptional activator required for lipid homeostasis, is directly transcriptionally repressed by FOXO1 (Deng et al. 2012). Transcription of the RETN gene, encoding resistin, an adipocyte specific hormone that suppresses insulin-mediated uptake of glucose by adipose cells, is directly stimulated by FOXO1 (Liu et al. 2014).

Transcription of two genes encoding E3 ubiquitin ligases FBXO32 (Atrogin-1) and TRIM63 (MURF1), involved in degradation of muscle proteins and muscle wasting during starvation, is positively regulated by FOXO transcription factors (Sandri et al. 2004, Waddell et al. 2008, Raffaello et al. 2010, Senf et al. 2011, Bollinger et al. 2014, Wang et al. 2017).

References

Paap RH, Oosterbroek S, Wagemans CM, von Oerthel L, Schellevis RD, Vastenhouw-van der Linden AJ, ... Smidt MP (2016). FoxO6 affects Plxna4-mediated neuronal migration during mouse cortical development. Proc. Natl. Acad. Sci. U.S.A.. ↗

Kops GJ, de Ruiter ND, De Vries-Smits AM, Powell DR, Bos JL & Burgering BM (1999). Direct control of the Forkhead transcription factor AFX by protein kinase B. Nature, 398, 630-4. ↗

Kops GJ, Dansen TB, Polderman PE, Saarloos I, Wirtz KW, Coffer PJ, ... Burgering BM (2002). Forkhead transcription factor FOXO3a protects quiescent cells from oxidative stress. Nature, 419, 316-21. ↗

Hori YS, Kuno A, Hosoda R & Horio Y (2013). Regulation of FOXOs and p53 by SIRT1 modulators under oxidative stress. PLoS ONE, 8, e73875. ↗

Araujo J, Breuer P, Dieringer S, Krauss S, Dorn S, Zimmermann K, ... Evert BO (2011). FOXO4-dependent upregulation of superoxide dismutase-2 in response to oxidative stress is impaired in spinocerebellar ataxia type 3. Hum. Mol. Genet., 20, 2928-41. ↗

Edit history

Date	Action	Author
2018-07-31	Created	Orlic-Milacic M
2018-10-11	Authored	Orlic-Milacic M

Date	Action	Author
2018-10-17	Reviewed	Donlon T
2018-10-26	Reviewed	Bertaggia E
2018-10-31	Edited	Orlic-Milacic M
2019-03-08	Modified	Weiser D

Entities found in this pathway (7)

Input	UniProt Id	#FC
PLXNA4	Q9HCM2	2.9
ABCA6	Q8N139	1.02
FOXO1	Q12778	2.31
INS-IGF2	P01308	-5.88e+00
FBXO32	Q969P5	1.09
FOXO3	O43524	1.26
NR3C1	P04150	-1.01e+00

Input	Ensembl Id	#FC
PLXNA4	ENSG00000221866	2.9
ABCA6	ENSG00000154262	1.02
FBXO32	ENSG00000156804	1.09

Interactors found in this pathway (3)

Input	UniProt Id	Interacts with	#FC
PPARG	P37231	Q9UBK2	1.03
ARHGEF2	Q92974	O43524	-1.02e+00
KLHL42	Q9P2K6	P01189	1.04

16. Diseases associated with O-glycosylation of proteins (R-HSA-3906995)
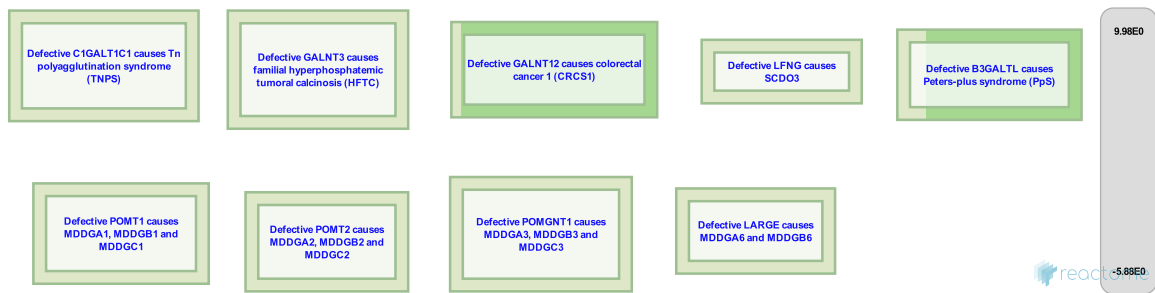
Diseases: congenital disorder of glycosylation.

Glycosylation is the most abundant modification of proteins, variations of which occur in all living cells. Glycosylation can be further categorized into N-linked (where the oligosaccharide is conjugated to Asparagine residues) and O-linked glycosylation (where the oligosaccharide is conjugated to Serine, Threonine and possibly Tyrosine residues). Within the family of O-linked glycosylation, the oligosaccharides attached can be further categorized according to their reducing end residue: Gal-NAc (often described as mucin-type, due to the abundance of this type of glycosylation on mucins), Mannose and Fucose. This section reviews currently known congenital disorders of glycosylation associated with defects of protein O-glycosylation (Cylwik et al. 2013, Freeze et al. 2014).

References

Cylwik B, Lipartowska K, Chrostek L & Gruszewska E (2013). Congenital disorders of glycosylation. Part II. Defects of protein O-glycosylation. Acta Biochim. Pol., 60, 361-8.

Freeze HH, Chong JX, Bamshad MJ & Ng BG (2014). Solving glycosylation disorders: fundamental approaches reveal complicated pathways. Am. J. Hum. Genet., 94, 161-75.

Edit history

Date	Action	Author
2013-07-17	Edited	Jassal B
2013-07-17	Authored	Jassal B
2013-07-17	Created	Jassal B
2015-12-18	Reviewed	Hansen L, Joshi HJ
2016-07-30	Modified	Gillespie ME

Entities found in this pathway (7)

Input	UniProt Id	#FC
ADAMTS1	Q9UHI8	2.28
ADAMTS14	Q8WXS8	-2.42e+00
ADAMTSL1	Q8N6G6	-1.05e+00
ADAMTS5	Q9UNA0	2.12
GALNT12	Q8IXK2	-1.16e+00
SPON1	Q9HCB6	1.8
THBS1	P07996	1.94

17.   Post-chaperonin tubulin folding pathway ([R-HSA-389977](R-HSA-389977))
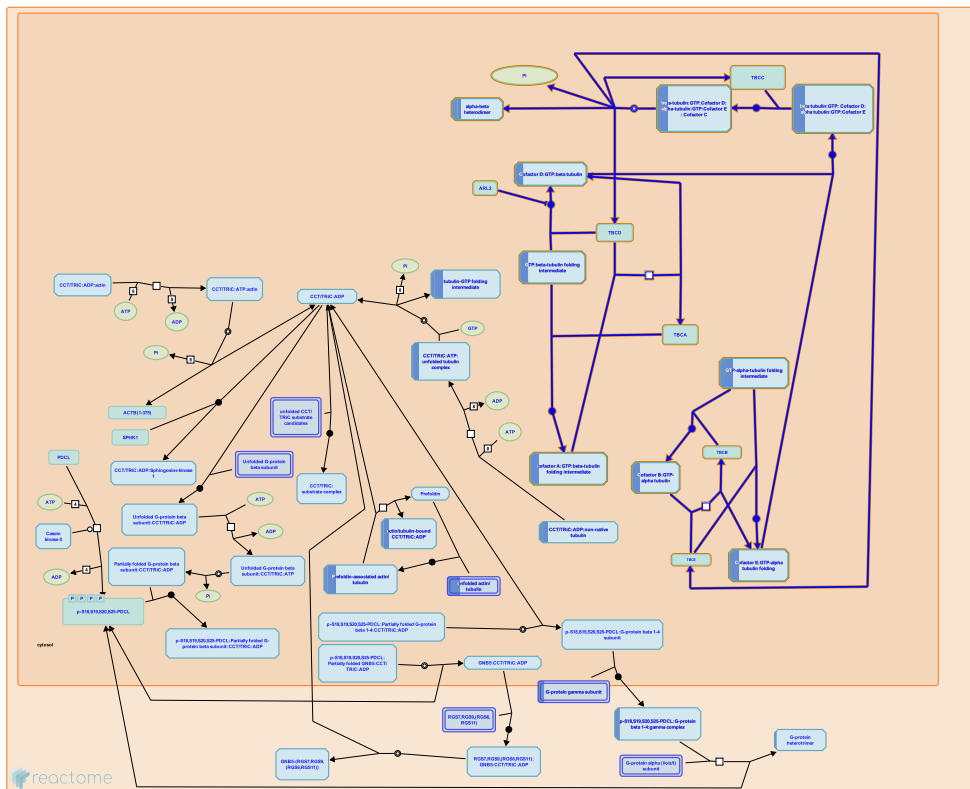
Cellular compartments: cytosol.

Alpha and beta tubulin folding intermediates are formed through ATP-dependent interaction with TriC/CCT. In order to form a functional heterodimer, these folding intermediates undergo a series of interactions with five proteins: (cofactors A-E) following release from TriC/CCT (reviewed in Cowan and Lewis et al., 2001). These interactions are described in the reactions below. Ultimately, alpha tubulin, when associated with cofactor E, interacts with cofactor D-bound beta-tubulin. The entry of cofactor C into this complex results in the discharge of native heterodimer triggered by GTP hydrolysis in beta tubulin (Tian et al., 1997).

References

Lewis SA, Tian G & Cowan NJ (1997). The alpha- and beta-tubulin folding pathways. Trends Cell Biol , 7, 479-84.

Edit history

Date	Action	Author
2008-12-01	Authored	Matthews L
2009-01-21	Reviewed	Cowan NJ
2009-01-22	Created	Matthews L
2009-02-21	Edited	Matthews L
2017-04-03	Modified	Matthews L

Entities found in this pathway (3)

Input	UniProt Id	#FC
TUBA4A	P68363, P68366	-1.45e+00
TUBB3	Q13509	-1.49e+00
TUBA1A	P68363, Q71U36	-1.29e+00

18. O-linked glycosylation ([R-HSA-5173105](R-HSA-5173105))
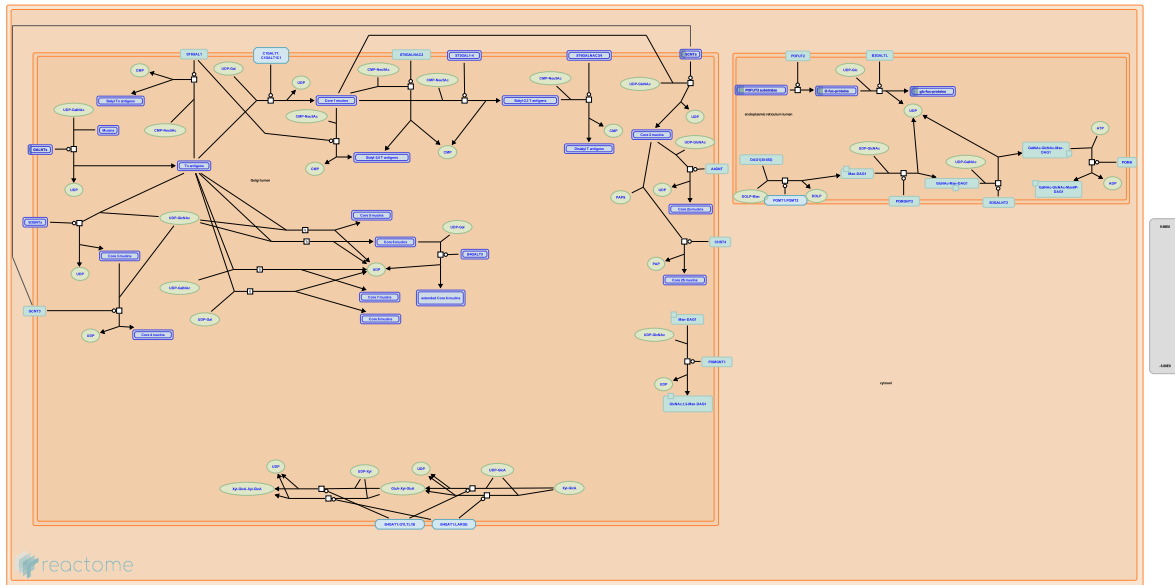
O-glycosylation is an important post-translational modification (PTM) required for correct functioning of many proteins (Van den Steen et al. 1998, Moremen et al. 2012). The O-glycosylation of proteins containing thrombospondin type 1 repeat (TSR) domains and O-glycosylation of mucins are currently described here.

References

Van den Steen P, Rudd PM, Dwek RA & Opdenakker G (1998). Concepts and principles of O-linked glycosylation. Crit. Rev. Biochem. Mol. Biol., 33, 151-208. ↗

Moremen KW, Tiemeyer M & Nairn AV (2012). Vertebrate protein glycosylation: diversity, synthesis and function. Nat. Rev. Mol. Cell Biol., 13, 448-62. ↗

Edit history

Date	Action	Author
2013-11-25	Edited	Jassal B
2013-11-25	Authored	Jassal B
2013-11-25	Created	Jassal B
2014-02-07	Reviewed	D'Eustachio P
2019-03-08	Modified	Weiser D

Entities found in this pathway (10)

Input	UniProt Id	#FC
GCNT4	Q9P109	1.97
ADAMTS1	Q9UHI8	2.28
GALNT16	Q8N428	-1.06e+00
ADAMTS14	Q8WXS8	-2.42e+00
GALNT15	Q7Z4T8, Q8N3T1	1.54
ADAMTSL1	Q8N6G6	-1.05e+00
ADAMTS5	Q9UNA0	2.12

Input	UniProt Id	#FC
GALNT12	Q8IXK2	-1.16e+00
SPON1	Q9HCB6	1.8
THBS1	P07996	1.94

Interactors found in this pathway (1)

Input	ChEBI Id	Interacts with	#FC
FAM20A	Q96MK3	15422	1.09

19. Activation of AMPK downstream of NMDARs (R-HSA-9619483)
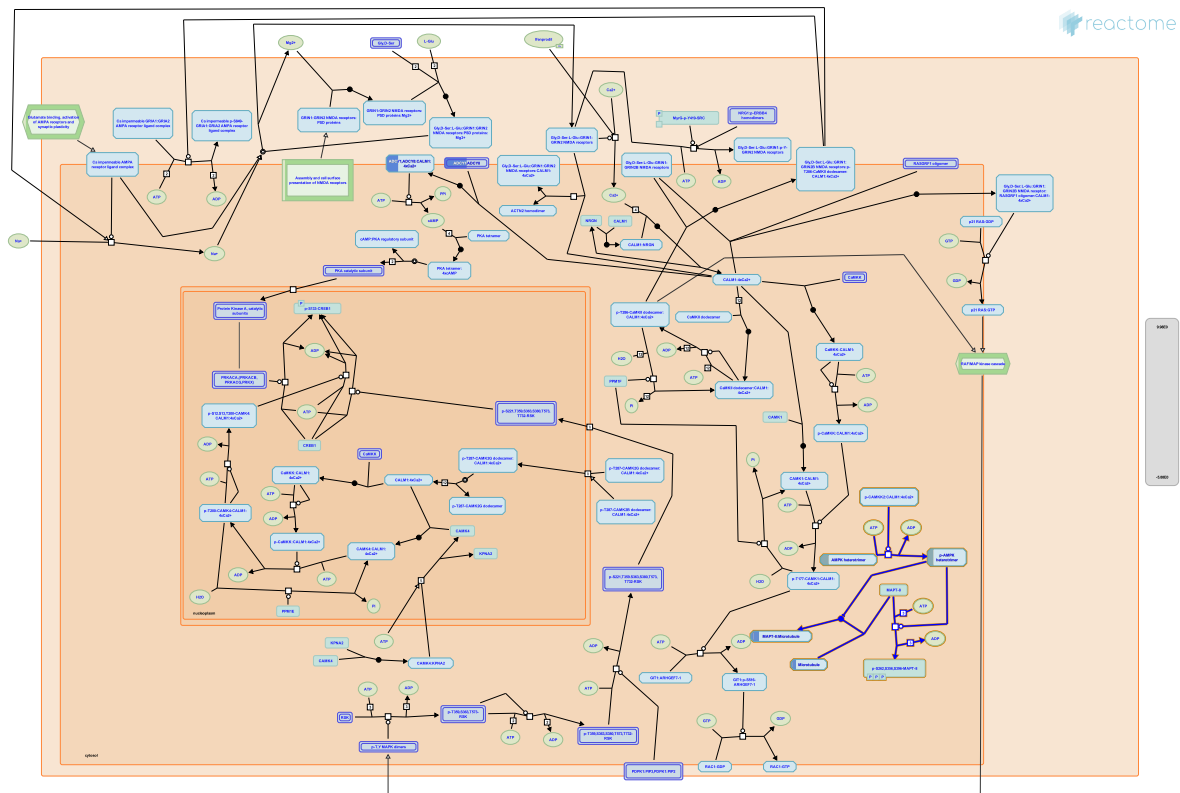
Cellular compartments: cytosol.

Activation of NMDA receptors (NMDARs) leads to activation of AMP-activated kinase (AMPK) in a CAMKK2-dependent manner. Overactivation of CAMKK2 or AMPK in neurons can lead to dendritic spine loss and is implicated in synaptotoxicity of beta-amyloids in Alzheimer's disease (Mairet-Coello et al. 2013).

References

Mairet-Coello G, Courchet J, Pieraut S, Courchet V, Maximov A & Polleux F (2013). The CAMKK2-AMPK kinase pathway mediates the synaptotoxic effects of A oligomers through Tau phosphorylation. Neuron, 78, 94-108.

Edit history

Date	Action	Author
2018-09-18	Created	Orlic-Milacic M
2018-10-11	Authored	Orlic-Milacic M
2018-11-02	Reviewed	Hansen KB, Yi F
2018-11-07	Edited	Orlic-Milacic M
2019-03-13	Modified	Weiser D

Entities found in this pathway (4)

Input	UniProt Id	#FC
PRKAG2	P54619, Q9UGJ0	1.57
TUBA4A	P68363, P68366	-1.45e+00

Input	UniProt Id	#FC
TUBB3	Q13509	-1.49e+00
TUBA1A	P68363, Q71U36	-1.29e+00

Interactors found in this pathway (1)

Input	ChEBI Id	Interacts with	#FC
FAM20A	Q96MK3	15422	1.09

20. Assembly of collagen fibrils and other multimeric structures (R-HSA-2022090)
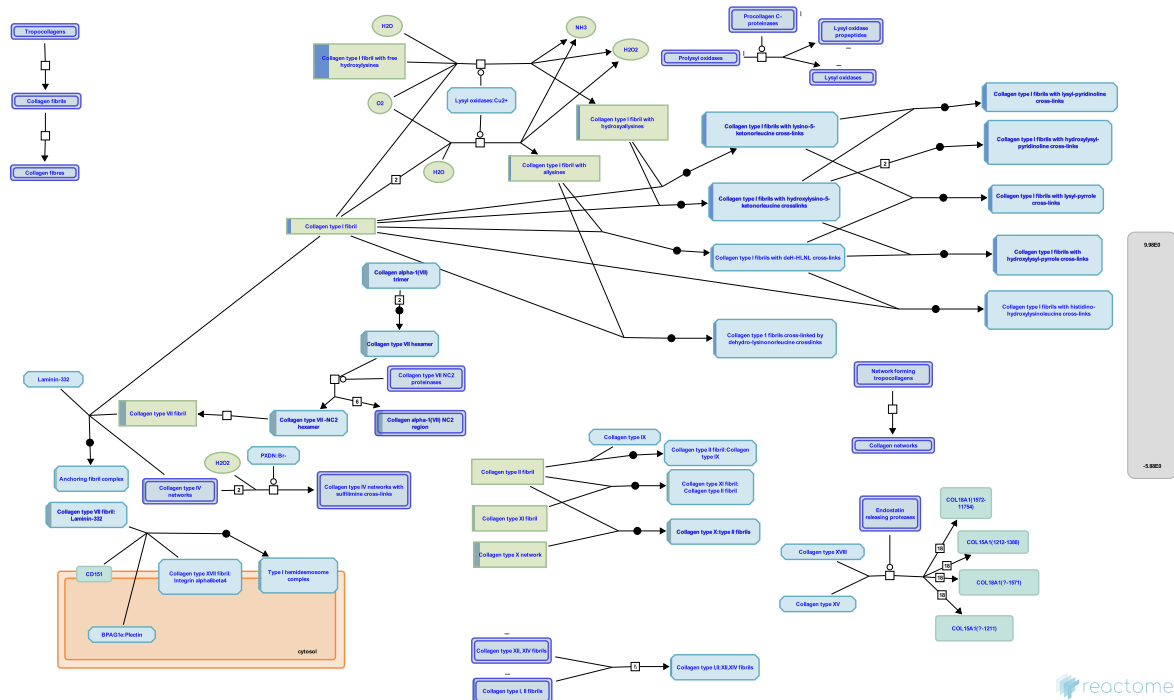
Collagen trimers in triple-helical form, referred to as procollagen or collagen molecules, are exported from the ER and trafficked through the Golgi network before secretion into the extracellular space. For fibrillar collagens namely types I, II, III, V, XI, XXIV and XXVII (Gordon & Hahn 2010, Ricard-Blum 2011) secretion is concomitant with processing of the N and C terminal collagen propeptides. These processed molecules are known as tropocollagens, considered to be the units of higher order collagen structures. They form within the extracellular space via a process that can proceed spontaneously, but in the cellular environment is regulated by many collagen binding proteins such as the FACIT (Fibril Associated Collagens with Interrupted Triple helices) family collagens and Small Leucine-Rich Proteoglycans (SLRPs). The architecture formed ultimately depends on the collagen subtype and the cellular conditions. Structures include the well-known fibrils and fibres formed by the major structural collagens type I and II plus several different types of supramolecular assembly (Bruckner 2010). The mechanical and physical properties of tissues depend on the spatial arrangement and composition of these collagen-containing structures (Kadler et al. 1996, Shoulders & Raines 2009, Birk & Bruckner 2011).

Fibrillar collagen structures are frequently heterotypic, composed of a major collagen type in association with smaller amounts of other types, e.g. type I collagen fibrils are associated with types III and V, while type II fibrils frequently contain types IX and XI (Wess 2005). Fibres composed exclusively of a single collagen type probably do not exist, as type I and II fibrils require collagens V and XI respectively as nucleators (Kadler et al. 2008, Wenstrup et al. 2011). Much of the structural understanding of collagen fibrils has been obtained with fibril-forming collagens, particularly type I, but some central features are believed to apply to at least the other fibrillar collagen subtypes (Wess 2005). Fibril diameter and length varies considerably, depending on the tissue and collagen types (Fang et al. 2012). The reasons for this are poorly understood (Wess 2005).

Some tissues such as skin have fibres that are approximately the same diameter while others such as tendon or cartilage have a bimodal distribution of thick and thin fibrils. Mature type I collagen fibrils in tendon are up to 1 cm in length, with a diameter of approx. 500 nm. An individual fibrillar collagen triple helix is less than 1.5 nm in diameter and around 300 nm long; collagen molecules must assemble to give rise to the higher-order fibril structure, a process known as fibrillogenesis, prevented by the presence of C-terminal propeptides (Kadler et al. 1987). In electron micrographs, fibrils have a banded appearance, due to regular gaps where fewer collagen molecules overlap, which occur because the fibrils are aligned in a quarter-stagger arrangement (Hodge & Petruska 1963). Collagen microfibrils are believed to have a quasi-hexagonal unit cell, with tropocollagen arranged to form supertwisted, right-handed microfibrils that interdigitate with neighbouring microfibrils, leading to a spiral-like structure for the mature collagen fibril (Orgel et al. 2006, Holmes & Kadler 2006).

Neighbouring tropocollagen monomers interact with each other and are cross-linked covalently by lysyl oxidase (Orgel et al. 2000, Maki 2006). Mature collagen fibrils are stabilized by lysyl oxidase-mediated cross-links. Hydroxylysyl pyridinoline and lysyl pyridinoline cross-links form between (hydroxy) lysine and hydroxylysine residues in bone and cartilage (Eyre et al. 1984). Arginoline cross-links can form in cartilage (Eyre et al. 2010); mature bovine articular cartilage contains roughly equimolar amounts of arginoline and hydroxylysyl pyridinoline based on peptide yields. Mature collagen fibrils in skin are stabilized by the lysyl oxidase-mediated cross-link histidino-hydroxylysinonorleucine (Yamauch et al. 1987). Due to the quarter-staggered arrangement of collagen molecules in a fibril, telopeptides most often interact with the triple helix of a neighbouring collagen molecule in the fibril, except for collagen molecules in register staggered by 4D from another collagen molecule. Fibril aggregation in vitro can be unipolar or bipolar, influenced by temperature and levels of C-proteinase, suggesting a role for the N- and C- propeptides in regulation of the aggregation process (Kadler et al. 1996). In vivo, collagen molecules at the fibril surface may retain their N-propeptides, suggesting that this may limit further accretion, or alternatively represents a transient stage in a model whereby fibrils grow in diameter through a cycle of deposition, cleavage and further deposition (Chapman 1989).

In vivo, fibrils are often composed from more than one type of collagen. Type III collagen is found associated with type I collagen in dermal fibrils, with the collagen III on the periphery, suggesting a regulatory role (Fleischmajer et al. 1990). Type V collagen associates with type I collagen fibrils, where it may limit fibril diameter (Birk et al. 1990, White et al. 1997). Type IX associates with the surface of narrow diameter collagen II fibrils in cartilage and the cornea (Wu et al. 1992, Eyre et al. 2004). Highly specific patterns of crosslinking sites suggest that collagen IX functions in interfibrillar networking (Wess 2005). Type XII and XIV collagens are localized near the surface of banded collagen I fibrils (Nishiyama et al. 1994). Certain fibril-associated collagens with interrupted triple helices (FACITs) associate with the surface of collagen fibrils, where they may serve to limit fibril fusion and thereby regulate fibril diameter (Gordon & Hahn 2010). Collagen XV, a member of the multiplexin family, is almost exclusively associated with the fibrillar collagen network, in very close proximity to the basement membrane. In human tissues collagen XV is seen linking banded collagen fibers subjacent to the basement membrane (Amenta et al. 2005). Type XIV collagen, SLRPs and discoidin domain receptors also regulate fibrillogenesis (Ansorge et al. 2009, Kalamajski et al. 2010, Flynn et al. 2010).

Collagen IX is cross-linked to the surface of collagen type II fibrils (Eyre et al. 1987). Type XII and XIV collagens are found in association with type I (Walchli et al. 1994) and type II (Watt et al. 1992, Eyre 2002) fibrils in cartilage. They are thought to associate non-covalently via their COL1/NC1 domains (Watt et al. 1992, Eyre 2002).

Some non-fibrillar collagens form supramolecular assemblies that are distinct from typical fibrils. Collagen VII forms anchoring fibrils, composed of antiparallel dimers that connect the dermis to the epidermis (Bruckner-Tuderman 2009). During fibrillogenesis, the nascent type VII procollagen molecules dimerize in an antiparallel manner. The C-propeptides are then removed by Bone morphogenetic protein 1 (Rattenholl et al. 2002) and the processed antiparallel dimers aggregate laterally. Collagens VIII and X form hexagonal networks and collagen VI forms beaded filament (Gordon & Hahn 2010, Ricard-Blum et al. 2011).

References

Kadler KE, Holmes DF, Trotter JA & Chapman JA (1996). Collagen fibril formation. Biochem J, 316, 1-11. ⬀

Orgel JP, San Antonio JD & Antipova O (2011). Molecular and structural mapping of collagen fibril interactions. Connect. Tissue Res., 52, 2-17. ⬀

Edit history

Date	Action	Author
2011-08-05	Authored	Jupe S
2011-11-25	Created	Jupe S
2012-10-08	Reviewed	Kalamajski S, Raleigh S
2012-11-12	Edited	Jupe S
2012-11-19	Reviewed	Ricard-Blum S
2019-03-08	Modified	Weiser D

Entities found in this pathway (5)

Input	UniProt Id	#FC
COL7A1	Q02388	1.22
COL4A4	P53420	2.02
COL4A1	P02462, Q03692	1.33
COL11A1	P12107	2.36
COL1A1	P02452	-1.31e+00

21. Crosslinking of collagen fibrils (R-HSA-2243919)
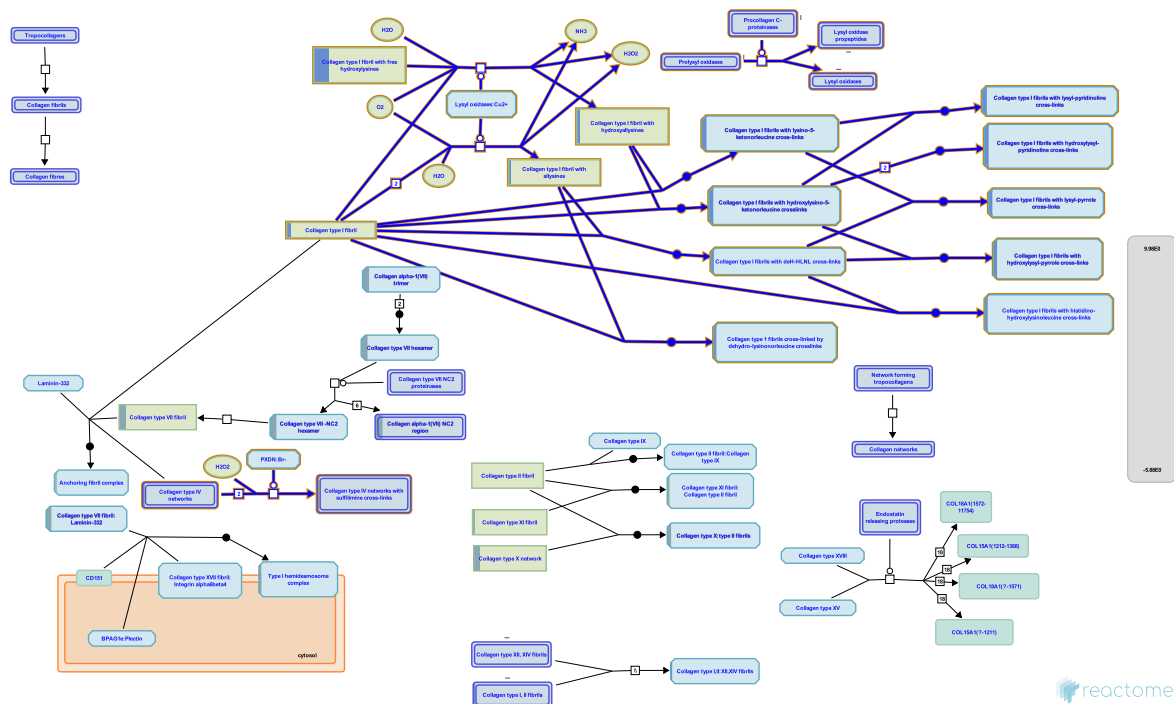
After removal of the N- and C-procollagen propeptides, fibrillar collagen molecules aggregate into microfibrillar arrays, stabilized by covalent intermolecular cross-links. These depend on the oxidative deamination of specific lysine or hydroxylysine residues in the telopeptide region by lysyl oxidase (LOX) with the subsequent spontaneous formation of covalent intermolecular cross-links (Pinnell & Martin 1968, Siegel et al. 1970, 1974, Maki 2009, Nishioka et al. 2012). Hydroxylysine is formed intracellularly by lysine hydroxylases (LH). There are different forms of LH responsible for hydroxylation of helical and telopeptide lysines (Royce & Barnes 1985, Knott et al.1997, Takaluoma et al. 2007, Myllyla 2007). The chemistry of the cross-links formed depends on whether lysines or hydroxylysines are present in the telopeptides (Barnes et al. 1974), which depends on the proportion of collagen lysines post-translationally converted to hydroxylysine by LH. The lysine pathway predominates in adult skin, cornea and sclera while the hydroxylysine pathway occurs primarily in bone, cartilage, ligament, tendons, embryonic skin and most connective tissues (Eyre 1987, Eyre & Wu 2005, Eyre et al. 2008). Oxidative deamination of lysine or hydroxylysine residues by LOX generates the allysine and hydroxyallysine aldehydes respectively. These can spontaneously react with either another aldehyde to form an aldol condensation product (intramolecular cross-link), or with an unmodified lysine or hydroxylysine residue to form intermolecular cross-links.

The pathway of cross-linking is regulated primarily by the hydroxylation pattern of telopeptide and triple-helix domain lysine residues. When lysine residues are the source of aldehydes formed by lysyl oxidase the allysine cross-linking pathway leads to the formation of aldimine cross-links (Eyre & Wu 2005). These are stable at physiological conditions but readily cleaved at acid pH or elevated temperature. When hydroxylysine residues are the source of aldehydes formed by lysyl oxidase the hydroxyallysine cross-linking pathway leads to the formation of more stable ketoimine cross-links.

Telopeptide lysine residues can be converted by LOX to allysine, which can react with a helical hydroxylysine residue forming the lysine aldehyde aldimine cross-link dehydro hydroxylysino norleucine (deHHLNL) (Bailey & Peach 1968, Eyre et al. 2008). If the telopeptide residue is hydroxylysine, the hydroxyallysine formed by LOX can react with a helical hydroxylysine forming the Schiff base, which spontaneously undergoes an Amadori rearrangement resulting in the ketoimine cross link hydroxylysino 5 ketonorleucine (HLKNL). This stable cross-link is formed in tissues where telopeptide residues are predominanly hydroxylated, such as foetal bone and cartilage, accounting for the relative insolubility of collagen from these tissues (Bailey et al. 1998). In bone, telopeptide hydroxyallysines can react with the epsilon-amino group of a helical lysine (Robins & Bailey 1975). The resulting Schiff base undergoes Amadori rearrangement to form lysino-hydroxynorleucine (LHNL). An alternative mechanism of maturation of ketoimine cross-links has been reported in cartilage leading to the formation of arginoline (Eyre et al. 2010).

These divalent crosslinks greatly diminish as connective tissues mature, due to further spontaneous reactions (Bailey & Shimokomaki 1971, Robins & Bailey 1973) with neighbouring peptides that result in tri- and tetrafunctional cross-links. In mature tissues collagen cross-links are predominantly trivalent. The most common are pyridinoline or 3-hydroxypyridinium cross-links, namely hydroxylysyl-pyridinoline (HL-Pyr) and lysyl-pyridinoline (L-Pyr) cross-links (Eyre 1987, Ogawa et al. 1982, Fujimoto et al. 1978). HL-Pyr is formed from three hydroxylysine residues, HLKNL plus a further hydroxyallysine. It predominates in highly hydroxylated collagens such as type II collagen in cartilage. L-Pyr is formed from two hydroxylysines and a lysine, LKNL plus a further hydroxyallysine, found mostly in calcified tissues (Bailey et al. 1998). Trivalent collagen cross-links can also form as pyrroles, either Lysyl-Pyrrole (L-Pyrrole) or hydroxylysyl-pyrrole (HL-Pyrrole), respectively formed when LKNL or HLKNL react with allysine (Scott et al. 1981, Kuypers et al. 1992). A further three-way crosslink can form when DeH-HLNL reacts with histidine to form histidino-hydroxylysinonorleucine (HHL), found in skin and cornea (Yamauchi et al. 1987, 1996). This can react with an additional lysine to form the tetrafunctional cross-link histidinohydroxymerodesmosine (Reiser et al. 1992, Yamauchi et al. 1996).

Another mechanism which could be involved in the cross-linking of collagen IV networks is the sulfimine bond (Vanacore et al. 2009), catalyzed by peroxidasin, an enzyme found in basement membrane (Bhave 2012).

To improve clarity inter-chain cross-linking is represented here for Collagen type I only. Although the formation of each type of cross-link is represented here as an independent event, the partial and random nature of lysine hydroxylation and subsequent lysyl oxidation means that any combination of these cross-linking events could occur within the same collagen fibril .

References

Bailey AJ, Paul RG & Knott L (1998). Mechanisms of maturation and ageing of collagen. Mech Ageing Dev, 106, 1-56. ↪

Edit history

Date	Action	Author
2012-04-30	Authored	Jupe S
2012-05-09	Created	Jupe S
2012-10-08	Reviewed	Kalamajski S, Raleigh S

Date	Action	Author
2012-11-12	Edited	Jupe S
2012-11-19	Reviewed	Ricard-Blum S
2019-03-08	Modified	Weiser D

Entities found in this pathway (3)

Input	UniProt Id	#FC
COL4A4	P53420	2.02
COL4A1	P02462	1.33
COL1A1	P02452	-1.31e+00

22.   Molecules associated with elastic fibres (R-HSA-2129379)

Proteins found associated with microfibrils include vitronectin (Dahlback et al. 1990), latent transforming growth factor beta-binding proteins (Kielty et al. 2002, Munger & Sheppard 2011), emilin (Bressan et al. 1993, Mongiat et al. 2000), members of the microfibrillar-associated proteins (MFAPs, Gibson et al.1996), and fibulins (Roark et al. 1995, Yanagisawa et al. 2002). The significance of these interactions is not well understood but may help mediate elastin-fibrillin interactions during elastic fibre assembly.

Proteoglycans such as versican (Isogai et al. 2002), biglycan, and decorin (Reinboth et al. 2002) can interact with the microfibrils. They confer specific properties including hydration, impact absorption, molecular sieving, regulation of cellular activities, mediation of growth factor association, and release and transport within the extracellular matrix (Buczek-Thomas et al. 2002). In addition, glycosaminoglycans have been shown to interact with tropoelastin through its lysine side chains (Wu et al. 1999) regulating tropoelastin assembly (Tu and Weiss, 2008).

References

Wagenseil JE & Mecham RP (2007). New insights into elastic fiber assembly. Birth Defects Res. C Embryo Today, 81, 229-40. ⮺

Kielty CM, Sherratt MJ & Shuttleworth CA (2002). Elastic fibres. J Cell Sci, 115, 2817-28. ⮺

Edit history

Date	Action	Author
2012-02-21	Created	Jupe S
2012-04-30	Authored	Jupe S
2012-11-02	Reviewed	Muiznieks LD
2012-11-12	Edited	Jupe S
2019-03-08	Modified	Weiser D

Entities found in this pathway (4)

Input	UniProt Id	#FC
FBN2	P35556	2.07
TGFB2	P61812	-1.62e+00
GDF5	P43026	-1.27e+00
ITGA8	P53708	1.07

23.   TGFBR2 MSI Frameshift Mutants in Cancer (R-HSA-3642279)
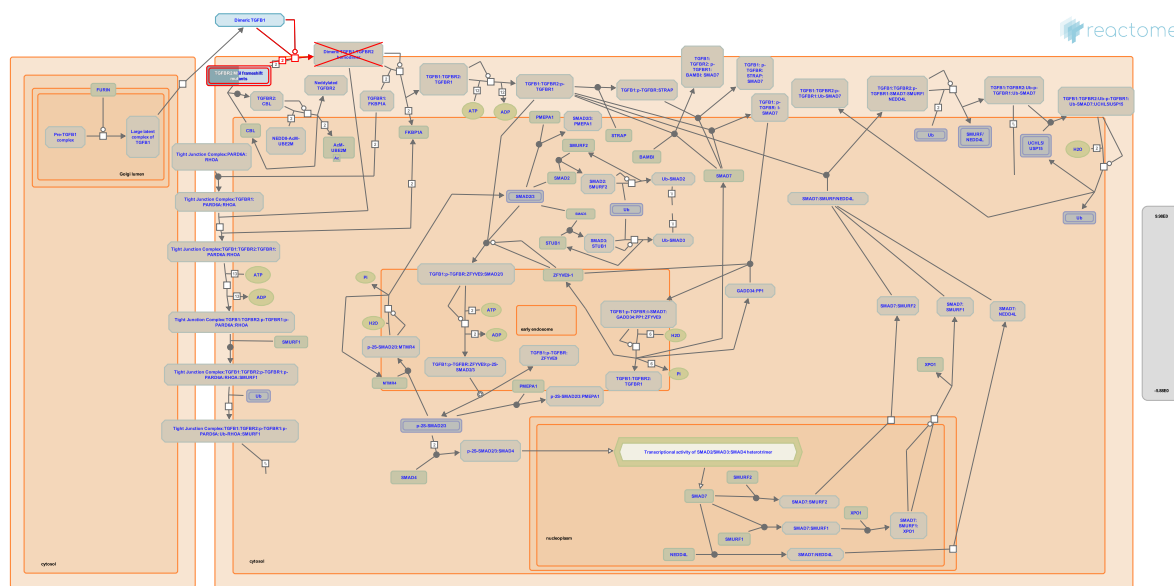
Diseases: cancer.

The short adenine repeat in the coding sequence of TGF-beta receptor II (TGFBR2) gene is frequently targeted by loss-of-function frameshift mutations in colon cancers with microsatellite instability (MSI). The 1- or 2-bp deletions in the adenine stretch of TGFBR2 cDNA introduce a premature stop codon that leads to degradation of the majority of mutant transcripts through nonsense-mediated decay or to production of a truncated TGFBR2 that cannot be presented on the cell surface. Cells that harbor TGFBR2 MSI frameshift mutations are resistant to TGF-beta (TGFB1)-mediated growth inhibition.

References

Markowitz S, Wang J, Myeroff L, Parsons R, Sun L, Lutterbaugh J, ... Vogelstein B (1995). Inactivation of the type II TGF-beta receptor in colon cancer cells with microsatellite instability. Science , 268, 1336-8. 🔗

Wang J, Sun L, Myeroff L, Wang X, Gentry LE, Yang J, ... Willson JK (1995). Demonstration that mutation of the type II transforming growth factor beta receptor inactivates its tumor suppressor activity in replication error-positive colon carcinoma cells. J. Biol. Chem., 270, 22044-9. 🔗

Edit history

Date	Action	Author
2013-05-31	Created	Orlic-Milacic M
2013-08-08	Edited	Orlic-Milacic M
2013-08-08	Reviewed	Meyer S, Akhurst RJ
2013-08-08	Authored	Meyer S, Akhurst RJ, Orlic-Milacic M
2019-03-13	Modified	Weiser D

Entities found in this pathway (1)

Input	UniProt Id	#FC
TGFBR2	P37173	1.44

24. VEGF ligand-receptor interactions (R-HSA-194313)
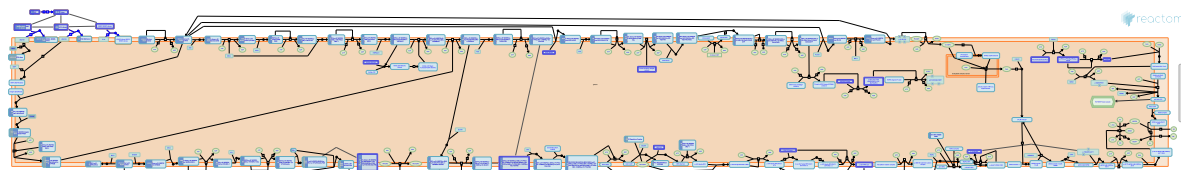
Cellular compartments: plasma membrane.

The VEGF family is encoded by seven genes (VEGF-A, B, C, D, E: PLGF (Placenta Growth Factor)-1, 2). Six isoforms of VEGF-A protein, containing 121, 145, 165, 183, 189, and 206 amino acid residues, and two isoforms of VEGF-B (167 and 186 residues) are specified by alternatively spliced mRNAs. The active form of each of these proteins is a homodimer.

The specificities of the three VEGF tyrosine kinase receptors, VEGFR-1, VEGFR-2 and VEGFR-3, for these ligands are shown in the figure (Hicklin and Ellis 2005). All VEGF-A isoforms bind both VEG-FR-1 and VEGFR-2; PLGF-1 and -2, and VEGF-B isoforms bind only VEGFR-1; VEGF-E binds VEGFR-2; and VEGF-C and -D bind both VEGFR-2 and -3. VEGF-D undergoes a complex series of post-translational modifications that results in secreted forms with increased activity toward VEGFR-3 and VEGFR-2.

Two co-receptor proteins in the cell membrane, neuropilin (NRP)-1 and NRP-2, interact with VEG-FR proteins to increase the affinity of the latter for their ligands (Neufeld et al.,2002). They differ from VEGFR proteins in not having intracellular signaling domains.

References

Olsson AK, Dimberg A, Kreuger J & Claesson-Welsh L (2006). VEGF receptor signalling - in control of vascular function. Nat Rev Mol Cell Biol, 7, 359-71. 🔗

Shibuya M & Claesson-Welsh L (2006). Signal transduction by VEGF receptors in regulation of angiogenesis and lymphangiogenesis. Exp Cell Res, 312, 549-60. 🔗

Matsumoto T & Mugishima H (2006). Signal transduction via vascular endothelial growth factor (VEGF) receptors and their roles in atherogenesis. J Atheroscler Thromb, 13, 130-5. 🔗

Cross MJ, Dixelius J, Matsumoto T & Claesson-Welsh L (2003). VEGF-receptor signal transduction. Trends Biochem Sci, 28, 488-94. 🔗

Edit history

Date	Action	Author
2007-03-13	Created	Gopinathrao G
2008-02-28	Reviewed	Claesson-Welsh L
2013-08-30	Edited	Garapati P V
2013-08-30	Authored	Garapati P V
2019-03-08	Modified	Weiser D

Entities found in this pathway (2)

Input	UniProt Id	#FC
PGF	P49763	-1.27e+00

Input	UniProt Id	#FC
VEGFA	P15692, P49765	-1.23e+00

Interactors found in this pathway (3)

Input	UniProt Id	Interacts with	#FC
PIK3R1	P27986	P17948	1.62
PGF	P49763	P17948	-1.27e+00
VEGFA	P15692-4	P35968, P17948	-1.23e+00

25.   VEGF binds to VEGFR leading to receptor dimerization (R-HSA-195399)
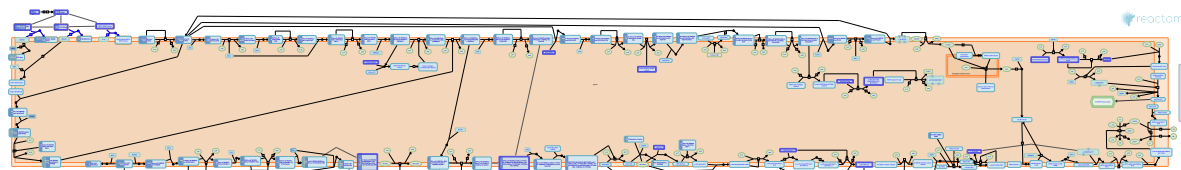
Cellular compartments: plasma membrane.

The binding of VEGF ligands to VEGFR receptors in the cell membrane induces dimerization and activation of the latter, initiating intracellular signaling cascades that result in proliferation, survival, migration and increased permeability of vascular endothelial cells (Matsumoto and Mugishima, 2006). The receptors predominantly form homodimers but heterodimers between VEGFR-1 and -2 have been observed. Although both VEGFR-1 and -2 are expressed in the vascular endothelium, the angiogenic activities of VEGFs are transduced mainly through VEGFR-2 in vivo.

References

Matsumoto T & Mugishima H (2006). Signal transduction via vascular endothelial growth factor (VEGF) receptors and their roles in atherogenesis. J Atheroscler Thromb, 13, 130-5.

Olsson AK, Dimberg A, Kreuger J & Claesson-Welsh L (2006). VEGF receptor signalling - in control of vascular function. Nat Rev Mol Cell Biol, 7, 359-71.

Cross MJ, Dixelius J, Matsumoto T & Claesson-Welsh L (2003). VEGF-receptor signal transduction. Trends Biochem Sci, 28, 488-94.

Edit history

Date	Action	Author
2007-04-06	Created	Gopinathrao G
2008-02-28	Reviewed	Claesson-Welsh L
2013-08-30	Edited	Garapati P V
2013-08-30	Authored	Garapati P V
2019-03-08	Modified	Weiser D

Entities found in this pathway (2)

Input	UniProt Id	#FC
PGF	P49763	-1.27e+00
VEGFA	P15692, P49765	-1.23e+00

Interactors found in this pathway (3)

Input	UniProt Id	Interacts with	#FC
PIK3R1	P27986	P17948	1.62
PGF	P49763	P17948	-1.27e+00
VEGFA	P15692-4	P35968, P17948	-1.23e+00

6. Identifiers found

Below is a list of the input identifiers that have been found or mapped to an equivalent element in Reactome, classified by resource.

Entities (337)

Input	UniProt Id	#FC
AASS	Q9UDR5	1.09
ABAT	P80404	1.15
ABCA10	Q8WWZ4	-1.44e+00
ABCA6	Q8N139	1.02
ABCC9	O60706	1.02
ABHD5	Q8WTS1	1.06
ABLIM1	O14639	1.39
ACKR4	Q9NPB9	-1.46e+00
ACSL1	P33121	1.6
ACSS1	Q9NUB1	1.86
ACTA2	P62736, P63267	1.07
ACTG2	P63267	1.91
ADAM12	O43184	-1.84e+00
ADAMTS1	Q9UHI8	2.28
ADAMTS14	Q8WXS8	-2.42e+00
ADAMTS5	Q9UNA0	2.12
ADAMTSL1	Q8N6G6	-1.05e+00
ADARB1	P78563	2.29
ADAT2	Q7Z6V5	-1.11e+00
ADCY1	Q08828	-2.24e+00
ADH1B	P00325	1.18
ADHFE1	Q8IWW8	1.42
ADM2	Q7Z4H4	-2.59e+00
ADRA1B	P35368	3.74
AGTRAP	Q6RW13	1.08
AHCTF1	Q8WYP5	1.28
AKR1C1	P42330	1.06
ALDH1B1	P30837	1
ALDH6A1	Q02252	1.2
ALOX15B	O15296	9.98
AMOT	Q4VCS5-1	-2.25e+00
AMPH	P49418	1.14
ANPEP	P15144	1.07
ANXA4	P04156	1.17
AOX1	Q06278	1.45
AP1M1	Q9BXS5	1.08
AQP3	Q92482	-2.97e+00
ARHGAP28	Q9P2N2	-1.52e+00
ARHGAP29	Q52LW3	1.2
ARHGEF2	Q92974	-1.02e+00
ARHGEF28	Q8N1W1	1.06

Input	UniProt Id	#FC
ARMC8	Q8IUR7	1.33
ARSI	Q5FYB1	-1.70e+00
ASNS	P08243	-1.27e+00
ATF3	P18847	1.98
ATP10A	O60312	1.3
ATP2A2	P16615	1.37
AXIN2	Q9Y2T1	1.17
BDKRB1	P46663	-1.93e+00
BDKRB2	P30411	-2.00e+00
BRCA1	P38398	-1.20e+00
C1QTNF1	Q8NFI3	1.21
C7	P10643	3.2
C9orf3	Q8N6M6	1.09
CACNB2	Q08289	3.37
CARMIL1	Q5VZK9	1.17
CCKAR	P32238	-2.22e+00
CCNA2	P20248	1.09
CDC42EP3	Q9UKI2	1.5
CDH6	P55285	-1.31e+00
CDKN1A	P38936	-1.03e+00
CDKN2B	P42772	-1.50e+00
CDON	Q4KMG0	-1.63e+00
CEBPD	P49716	1.48
CFLAR	O15519-1, O15519-2	1.19
CH25H	O95992	-1.60e+00
CHST7	Q9NS84	1.56
CILP	O75339	1.35
CIT	O14578, O14578-3	-1.58e+00
CITED2	Q99967	1.6
CITED4	Q96RK1	1.44
CLDN11	O75508	-1.74e+00
CLIC2	O15247	-1.24e+00
COL11A1	P12107	2.36
COL1A1	P02452	-1.31e+00
COL4A1	P02462	1.33
COL4A4	P53420	2.02
COL7A1	Q02388	1.22
CORIN	Q9Y5Q5	1.93
COX11	Q9Y6N1	1.14
CPM	P14384	1.49
CRABP2	P29373	-1.69e+00
CREB3L1	Q96BA8	-1.01e+00
CRISPLD2	Q9H0B8	2.68
CTGF	P29279	1.37
CTPS1	P17812	1.51
CXCL12	P48061	-1.93e+00
CYFIP2	Q96F07	-1.00e+00
CYR61	O00622	1.8
CYTH3	O43739	1.18
DAAM1	Q9Y4D1	-1.02e+00

Input	UniProt Id	#FC
DAPK2	Q9UIK4	1.55
DCXR	Q7Z4W1	2.12
DDAH1	O94760	1.32
DDI2	Q92681	1.07
DDIT3	P35638	-1.05e+00
DHRS3	O75911	1.1
DIO2	Q92813	1.53
DLL4	Q9NR61	3.75
DNM1	Q05193	-1.74e+00
DOK6	Q6PKX4	-1.14e+00
DUSP1	P28562	2.94
DUSP10	Q9Y6W6	-1.22e+00
DUSP5	Q16690	1.28
EBF1	Q9UH73	1.12
ENDOD1	O94919	1.96
ENPP1	P22413	1.35
EPB41	P11171	-1.02e+00
EPHA4	P54764	1.35
EPHB2	P29323	-1.77e+00
EPHB3	P54753	-1.45e+00
EPHB6	O15197	1.29
FAM20A	Q96MK3	1.09
FBN2	P35556	2.07
FBXO32	Q969P5	1.09
FDXR	P22570	-1.00e+00
FGD4	Q96M96	2.26
FGF14	Q92915	1.11
FKBP5	Q13451	3.93
FLRT3	Q9NZU0	-2.35e+00
FOXO1	Q12778	2.31
FOXO3	O43524	1.26
FST	P19883	-1.78e+00
FSTL3	O95633	1.83
FZD8	Q9H461	2.44
G0S2	P27469	-2.73e+00
GALNT12	Q8IXK2	-1.16e+00
GALNT15	Q7Z4T8, Q8N3T1	1.54
GALNT16	Q8N428	-1.06e+00
GCH1	P30793	1.61
GCHFR	P30047	1.91
GCLM	P48507	1.24
GCNT4	Q9P109	1.97
GDF5	P43026	-1.27e+00
GDNF	P39905	1.83
GFPT2	O94808	1.3
GGT5	P36269	2.36
GLS	O94925	1.19
GLUL	P15104	2.99
GNG2	P50150, P59768	-1.11e+00
GPAT3	Q53EU6	1.21

Input	UniProt Id	#FC
GPR37	O15354	1.46
GPR68	Q15743	-3.20e+00
GPX3	O75715, P22352	3.72
HBA1	P69905	-3.38e+00
HIF3A	Q9Y2N7	2.53
HIGD1A	Q9Y241	1.19
HIST2H2AA4	Q6FI13	3.83
HMGB2	P26583	1.22
HMOX1	P09601	-1.35e+00
HPS5	P0DJI8	1.59
HSD17B6	O14756	-2.15e+00
HSPA12B	Q96MM6	-2.37e+00
HSPA2	P54652	2.55
HSPA4L	O95757	-1.28e+00
IER3	P46695	-1.18e+00
IFIT1	P09914	-1.63e+00
IGFBP2	P18065	2.05
IL12A	P29459	-2.01e+00
IL34	Q6ZMJ4	-2.10e+00
IMPA2	O14732	2.31
ING2	Q9H160	1.27
INHBA	P08476	1.07
INHBB	P09529	3.64
INPP5A	Q14642	1.37
INS-IGF2	P01308	-5.88e+00
IRS2	Q9Y4H2	2.15
ITGA10	O75578	3.83
ITGA11	Q9UKX5	-1.60e+00
ITGA2	P17301	-1.04e+00
ITGA8	P53708	1.07
ITGBL1	O95965	1.07
JADE1	Q6IE81	1.22
JUN	P05412	-1.08e+00
KANK1	Q14678	1.22
KCNE3	Q9Y6H6	-1.30e+00
KCNK15	Q9H427	-1.43e+00
KCNK6	Q9Y257	2.88
KLF15	Q9UIH9	4.56
KLF5	Q13887	2.55
KLHL42	Q9P2K6	1.04
LAMA2	P24043	2.07
LEP	P41159	3.28
LGR4	Q9BXB1	-1.10e+00
LHFPL2	Q6ZUX7	-1.26e+00
LIF	P15018	-2.54e+00
LIG1	P18858	-1.01e+00
LIMS2	Q7Z4I7	1.27
LMCD1	Q9NZU5	1.61
LMOD1	P29536	1.12
MAFF	Q9ULX9	1.26

Input	UniProt Id	#FC
MAOA	P21397	3.28
MAOB	P21397	1.22
MAP1LC3C	Q9BXW4	2.53
MAP3K8	P41279	1.12
MARCKS	P29966	-1.19e+00
METTL7A	Q9H8H3	2.31
MFGE8	Q08431	1.07
MMP15	P51511	1.28
MORF4L2	Q15014	1
MPST	P25325	1.01
MT1E	P04732	2.16
MT1M	P13640, Q8N339	2.4
MT1X	P80297	3.24
MT2A	P02795, P04731	2.19
MX1	P20591	-1.01e+00
NAMPT	P43490	1.03
NCOA3	Q9Y6Q9	1.41
NEDD4L	Q96PU5	-1.06e+00
NEGR1	Q7Z3B1	1.46
NF2	P35240	1.02
NFIL3	Q16649	1.14
NFYB	P25208	1.03
NID1	P14543	1.54
NNMT	P40261	2.15
NOV	Q9UIW2	-2.55e+00
NPAS2	Q99743	1.12
NR3C1	P04150-1, P04150-2, P04150-3, P04150-4, P04150-5, P04150-6, P04150-7, P04150-8, P04150-9	-1.01e+00
NR4A1	P22736	1.34
NR4A3	Q92570-1, Q92570-2	2.11
NRP2	O60462	1.03
NUAK1	O60285	1.37
OLFML1	Q8ND30	-1.02e+00
OMD	Q99983	1.79
OMG	P23515	-1.74e+00
OSBPL3	Q9H4L5	-1.09e+00
P2RX7	Q99572	-1.94e+00
PAFAH1B3	Q15102	-1.26e+00
PCYT2	Q99447	1.12
PDE5A	O76074	-1.17e+00
PDK4	Q16654	2.56
PDLIM5	Q96HC4	1.59
PDPN	Q86YL7	1.85
PER1	O15534	3.15
PGF	P49763	-1.27e+00
PHC2	Q8IXK0	1.37
PHGDH	O43175	-1.44e+00
PHLDA1	Q8WV24	-1.08e+00
PIK3R1	P27986	1.62

Input	UniProt Id	#FC
PIK3R3	Q92569	-1.70e+00
PLA2G4A	P47712	-2.45e+00
PLK2	Q9NYY3	-1.05e+00
PLPP3	O14495	-1.02e+00
PLXNA4	Q9HCM2	2.9
PNPLA2	Q96AD5	1.07
PPARG	P37231	1.03
PPP1CB	P62140	1.06
PPP1R14A	Q96A00	2.81
PPP1R1B	Q9UD71	-3.12e+00
PRDM1	O75626	1.26
PREB	Q9HCU5	1.11
PRKAG2	P54619, Q9UGJ0	1.57
PRKCE	Q02156	-1.23e+00
PRKG2	Q13237	-1.65e+00
PSAT1	Q9Y617	-1.28e+00
PTK2B	Q14289	1.11
PTX3	P26022	2.21
QPCT	Q16769	1.14
QPRT	Q15274	-1.23e+00
RAB7B	Q96AH8	-1.85e+00
RAC3	P60763	1.47
RAP2B	P61225	-1.28e+00
REV3L	O60673	1.12
RGCC	Q9H4X1	3.17
RGL1	Q9NZL6	-1.10e+00
RHOB	P62745	1.17
RHOBTB3	O94955	1.04
RHOJ	Q9H4E5	-1.20e+00
RNF144B	Q7Z419	2.2
RNF217	Q8TC41	1.08
ROBO1	Q9Y6N7	-1.14e+00
RSPO1	Q2MKA7	1.33
RSPO2	Q2I0M5, Q6UXX9	-1.48e+00
S1PR1	P21453	-1.47e+00
SAMHD1	Q9Y3Z3	3.84
SAP30	O75446	1.22
SAT1	Q9H2B4	1.32
SCD	O00767	-1.98e+00
SCN7A	Q01118	1.43
SEMA3A	Q14563	-1.22e+00
SEMA6D	Q8NFY4	-1.31e+00
SERPINA3	P01011	3.29
SLC19A2	O60779	1.1
SLC38A2	Q96QD8	1.23
SLC38A5	Q8WUX1	-1.01e+00
SLC39A10	Q9ULF5	-1.23e+00
SLC5A6	Q9Y289	1.2
SLC6A6	P31641	-2.10e+00
SLC6A9	P48067	-2.23e+00

Input	UniProt Id	#FC
SLC7A5	Q01650	-1.19e+00
SLC7A6	Q92536	1.64
SMARCD2	Q92925	1.26
SOCS1	O15524	-1.15e+00
SORT1	Q99523	2.21
SOX4	Q06945	-2.38e+00
SOX9	P48436	-1.28e+00
SPARCL1	Q14515	4.62
SPINT2	O43291	1.8
SPON1	Q9HCB6	1.8
SQOR	Q9Y6N5	1.01
STARD7	Q9NQZ5	1.24
STEAP2	Q8NFT2	1.98
STOM	P27105	1.42
STON1	Q9Y6Q2	1.38
SUN2	Q9UH99	1.88
SYDE2	Q5VT97	1.22
TGFB2	P61812	-1.62e+00
TGFBR2	P37173	1.44
THBS1	P07996	1.94
TJP2	Q9UDY2	1.97
TNFAIP6	P98066	-2.50e+00
TNFRSF11B	O00300, O95407	-1.54e+00
TNFSF13B	Q9Y275	-1.95e+00
TNIK	Q9UKE5	-1.15e+00
TRIB3	Q96RU7	-1.10e+00
TRIM45	Q9H8W5	-1.97e+00
TRPC6	Q9Y210	1.94
TSC22D3	Q99576	3.32
TSLP	Q969D9	-2.80e+00
TST	Q16762	1.29
TUBA1A	P68363, Q71U36	-1.29e+00
TUBA4A	P68363, P68366	-1.45e+00
TUBB	P07437	-1.21e+00
TUBB3	Q13509	-1.49e+00
TXNRD1	Q16881	1.53
TYMP	P19971	1.43
UNC5B	Q8IZJ1	-1.03e+00
VCAM1	P19320	-3.60e+00
VEGFA	P15692	-1.23e+00
WARS	P23381	-1.33e+00
WASF3	Q9UPY6	1.08
WNT2	P09544	-3.15e+00
ZBTB16	Q05516	7.05
ZCCHC6	Q5VYS8	1.11
ZNF135	P52742	-1.22e+00
ZNF521	Q96K83	-1.02e+00

Input	Ensembl Id	#FC
ABCA6	ENSG00000154262	1.02
ACSL1	ENSG00000151726	1.6
ACTA2	ENSG00000107796	1.07
ASNS	ENSG00000070669	-1.27e+00
ATF3	ENSG00000162772	1.98
AXIN2	ENSG00000168646, ENST00000307078	1.17
BRCA1	ENSG00000012048, ENST00000357654	-1.20e+00
CCNA2	ENSG00000145386	1.09
CDKN1A	ENSG00000124762	-1.03e+00
CDKN2B	ENSG00000147883	-1.50e+00
CEBPD	ENSG00000221869	1.48
CITED2	ENSG00000164442	1.6
COL1A1	ENSG00000108821	-1.31e+00
CTGF	ENSG00000118523	1.37
CXCL12	ENSG00000107562	-1.93e+00
DDIT3	ENSG00000175197	-1.05e+00
EBF1	ENSG00000164330	1.12
FBXO32	ENSG00000156804	1.09
FKBP5	ENSG00000096060	3.93
FOXO1	ENSG00000150907	2.31
FOXO3	ENSG00000118689	1.26
G0S2	ENSG00000123689	-2.73e+00
HIGD1A	ENSG00000181061	1.19
HMOX1	ENSG00000100292	-1.35e+00
IFIT1	ENSG00000185745	-1.63e+00
IL12A	ENSG00000168811	-2.01e+00
ITGBL1	ENSG00000198542	1.07
KLF15	ENSG00000163884	4.56
KLF5	ENSG00000102554	2.55
LEP	ENSG00000174697	3.28
LIF	ENSG00000128342	-2.54e+00
MAOA	ENSG00000189221	3.28
MT2A	ENSG00000125148	2.19
MX1	ENSG00000157601	-1.01e+00
NAMPT	ENSG00000105835	1.03
NPAS2	ENSG00000170485	1.12
NR4A3	ENSG00000119508	2.11
PER1	ENSG00000179094, ENST00000317276	3.15
PIK3R1	ENSG00000145675	1.62
PLK2	ENSG00000145632	-1.05e+00
PLXNA4	ENSG00000221866	2.9
PPARG	ENSG00000132170	1.03
PRDM1	ENSG00000057657	1.26
PREB	ENSG00000138073	1.11
RGCC	ENSG00000102760	3.17
RGL1	ENSG00000143344	-1.10e+00
ROBO1	ENSG00000169855	-1.14e+00
S1PR1	ENSG00000170989	-1.47e+00
SAMHD1	ENSG00000101347	3.84
SCD	ENSG00000099194	-1.98e+00

Input	Ensembl Id	#FC
SOCS1	ENSG00000185338	-1.15e+00
THBS1	ENSG00000137801	1.94
TNIK	ENSG00000154310	-1.15e+00
TRIB3	ENSG00000101255	-1.10e+00
TRIM45	ENSG00000134253	-1.97e+00
TSC22D1	ENSG00000102804	1.18
TXNRD1	ENSG00000198431	1.53
VCAM1	ENSG00000162692	-3.60e+00
VEGFA	ENSG00000112715	-1.23e+00

Interactors (225)

Input	UniProt Id	Interacts with	#FC
ABHD5	Q8WTS1	Q99541	1.06
ABLIM1	O14639-4	Q14192	1.39
ADAM12	O43184-2	O95633	-1.84e+00
ADARB1	P78563-4	P19525	2.29
AGTRAP	Q6RW13	Q00059	1.08
AKR1C1	Q04828	P26045	1.06
ALOX15B	O15296	P19474	9.98
AMOT	A2BDD9	Q14192	-2.25e+00
AMPH	P49418	Q05193	1.14
AP1M1	Q9BXS5	P18848	1.08
APBB2	Q92870	P00533	1.08
APCDD1	Q8J025	O75197	1.74
AQP3	Q92482	Q6IN84	-2.97e+00
ARHGEF2	Q92974	O43524	-1.02e+00
ARMC8	Q8IUR7	Q6VN20, Q96S59	1.33
ASNS	P08243	P11142	-1.27e+00
ATF3	P18847	P35638, P18847, P18848	1.98
ATP2A2	P16615	Q13418	1.37
AXIN2	Q9Y2T1	P49841	1.17
BRCA1	P38398	Q9ULW0, O75330	-1.20e+00
BRIX1	Q8TDN6	P62753	1.03
C1QTNF1	Q9BXJ1-2	P22735	1.21
C4orf46	Q504U0	Q9UL45	-1.38e+00
CACNB2	Q08289	O14744	3.37
CALCOCO2	Q13137	P30626	1.14
CARMIL1	Q5VZK9	Q00613	1.17
CBSL	P0DN79	O75928-2	1.36
CCDC107	Q8WV48	Q9H1C4	1
CCDC34	Q96HJ3-2	Q8N661	-1.29e+00
CCNA2	P20248	P38936	1.09
CD302	Q8IX05	Q3SXY8	1.82
CD82	P27701	O15552	1.26
CDC42EP3	Q9UKI2	Q5S007	1.5
CDKN1A	EBI-1550784	Q09472	-1.03e+00
CDKN2B	P42772	Q9UI12	-1.50e+00
CDON	Q4KMG0	P00519	-1.63e+00
CEBPD	P49716	Q9BXW9	1.48
CFLAR	O15519	Q14790	1.19

Input	UniProt Id	Interacts with	#FC
CHRDL2	Q6WN34-2	O75093	-1.44e+00
CITED2	Q99967	Q09472	1.6
CLDN11	O75508	P26715	-1.74e+00
COL1A1	P02452	P02751	-1.31e+00
COL7A1	Q02388	Q5JRA6	1.22
CORIN	Q9Y5Q5	O00501	1.93
CORO6	Q6QEF8	Q9UL45	2.34
CREB3L1	Q96BA8	P21854	-1.01e+00
CREB5	Q02930-3	P19883	-1.98e+00
CTGF	P29279	P02751	1.37
CTPS1	P17812	P01106	1.51
CTTNBP2	Q8WZ74	O43815	-1.08e+00
CXCL12	P48061	P78556, P13501, O15444, Q99616	-1.93e+00
CYFIP2	Q96F07	Q13485	-1.00e+00
CYR61	O00622	O60906	1.8
CYTH3	O43739-2	P53365	1.18
DAAM1	Q9Y4D1	Q9Y4D1	-1.02e+00
DAAM2	EBI-12904486	Q08426	1.66
DCXR	Q7Z4W1	Q7Z4W1	2.12
DDIT3	P35638	P18847, P18848	-1.05e+00
DNAJB4	Q9UDY4	Q9Y230	1.52
DNM1	Q05193	Q05193, 15996	-1.74e+00
DOK6	Q6PKX4	Q16288	-1.14e+00
DUSP1	P28562	Q16539	2.94
DUSP10	Q9Y6W6	P49639	-1.22e+00
DUSP23	Q9BVJ7	Q8TBC4	1.34
DUSP5	Q16690	P28482	1.28
EOGT	Q5NDL2-3	Q9UKG4	1.27
EPHB2	P54763	Q13009	-1.77e+00
EPHB6	O15197-2	Q96RU7	1.29
ERRFI1	Q9UJM3	P31947	2.42
EVI2A	P22794	Q9Y5Z9	-1.62e+00
FAM107A	O95990-4	Q12933	4.63
FAM46A	EBI-12149039	O14503	-1.15e+00
FAM46B	Q96A09	O14503	2.33
FBN2	P35556	P04608	2.07
FGF14	Q92915-2	P49638	1.11
FKBP5	Q13451	Q15831	3.93
FOXO1	Q12778	Q92793	2.31
FOXO3	O43524	Q92793	1.26
FST	P19883	P10599	-1.78e+00
FZD8	Q9H461	P56704	2.44
GADD45B	O75293	O14733	1.43
GALNT15	Q8N3T1	P30825	1.54
GAS2L3	Q86XJ1	Q96GD4	-1.10e+00
GCH1	P30793	P63104	1.61
GDF15	Q99988	Q13185	-1.86e+00
GFPT2	O94808	Q9NUX5	1.3
GNG2	P59768	P62873	-1.11e+00

Input	UniProt Id	Interacts with	#FC
GPM6B	P35803	P31645	2.63
GPR37	O15354	Q01959	1.46
GRAMD4	Q6IC98	Q96QG7	-1.18e+00
HBA1	P69905	P0DMV8	-3.38e+00
HMGB2	P26583	P48729	1.22
HMOX1	P09601	Q9NUX5	-1.35e+00
HSPA12B	Q96MM6	Q12933	-2.37e+00
HSPA2	P54652	P11142	2.55
HSPA4L	O95757	P11142	-1.28e+00
IER3	P46695	Q9UKG4	-1.18e+00
IFIT1	P09914	Q86WV6	-1.63e+00
IL12A	P29459	P29460	-2.01e+00
IL34	Q6ZMJ4-1	P07333	-2.10e+00
IMPA2	O14732	Q8TBC4	2.31
ING2	Q9H160	P12004	1.27
INS-IGF2	F8WCM5	P16150	-5.88e+00
IRS2	Q9Y4H2	Q96EB6	2.15
ITGA2	P17301	P05556	-1.04e+00
JADE1	Q6IE81	O75161	1.22
JUN	P05412	P18847, P18848	-1.08e+00
KANK1	Q14678	Q9UQB8	1.22
KIAA0408	Q6ZU52	O43639	1.5
KLF15	Q9UIH9	Q9UKG1	4.56
KLF5	Q13887	P0CG48	2.55
KLF6	Q99612	Q04206	1.09
KLHL42	Q9P2K6	P01189	1.04
LDB2	O43679	O00560	-1.32e+00
LHFPL2	Q6ZUX7	P08034	-1.26e+00
LIF	P15018	P40189	-2.54e+00
LIMS2	Q7Z4I7-5	Q96PM5	1.27
MAP1LC3C	Q9BXW4	Q96A56	2.53
MAP3K8	P41279	P19838, Q8NFZ5	1.12
MEST	Q5EB52	Q05329	-1.81e+00
MFSD6	Q6ZSS7	P29033	1.04
MMD	Q15546	Q3SXY8	1.64
MORF4L2	Q15014	Q99856	1
MPP3	Q13368	Q9HAP6	1.52
MPST	P25325	O96006	1.01
MX1	P20591	Q13507	-1.01e+00
MYADM	Q96S97	Q9Y624	1.48
NAMPT	P43490	P43490	1.03
NCOA3	Q9Y6Q9	Q09472, Q92793	1.41
NEDD4L	Q96PU5-5	O15105	-1.06e+00
NEDD9	Q14511	Q8IZD9	1.65
NEGR1	Q7Z3B1	P61916	1.46
NEK11	Q8NG66	P51955	-1.30e+00
NF2	P35240	Q8NI35	1.02
NFIL3	Q16649	P16220	1.14
NFYB	P25208	P04637	1.03
NKD2	Q969F2	Q96PM5	1.38

Input	UniProt Id	Interacts with	#FC
NOV	P48745	O43559	-2.55e+00
NPAS2	Q99743	O43639	1.12
NR3C1	P04150	P31948	-1.01e+00
NR4A1	P22736	Q9Y4D7	1.34
NR4A3	Q92570	Q9H2F3	2.11
NRP2	Q99435-2	P49639	1.03
NUAK1	O60285	P04637	1.37
OSBPL3	Q9H4L5	P31946	-1.09e+00
P2RX7	Q99572	P14373	-1.94e+00
PAFAH1B3	Q15102	P19320	-1.26e+00
PER1	J3QSH9	O15055	3.15
PER3	P56645	O96017	-2.25e+00
PGF	P49763	P17948	-1.27e+00
PHC2	Q8IXK0	P53350	1.37
PIK3R1	P27986-2, P27986	P48023, O15524	1.62
PIK3R3	Q92569	Q06187	-1.70e+00
PKIA	P61925	O43663	-1.34e+00
PLEKHG4	Q58EX7	Q9NQ94	-1.35e+00
PLPP3	O14495	O60716	-1.02e+00
PPARG	P37231	Q9UBK2	1.03
PPP1CB	P62140	Q9UQK1	1.06
PPP1R14A	Q96A00	P48729	2.81
PPTC7	Q8NI37	P41182	1.19
PRDM1	O75626	O75925	1.26
PRKCE	Q02156	P08238	-1.23e+00
PRR5L	Q6MZQ0	Q14192	1.61
PTK2B	Q14289	P06241	1.11
PTX3	P26022	P09038	2.21
QPRT	Q15274	Q15274	-1.23e+00
RAC3	Q9Y6Q9	Q09472, Q92793	1.47
RAP2B	P61225	P19320	-1.28e+00
RASD1	Q9Y272	O75525	2.17
RASSF2	P50749	O60341	-1.09e+00
REV3L	O60673	Q9UI95	1.12
RHOBTB3	O94955	O14503	1.04
RHOJ	Q9H4E5	Q13177	-1.20e+00
RNF144B	Q7Z419	Q07812	2.2
ROBO1	Q9Y6N7	O75044	-1.14e+00
RSPO2	Q6UXX9-2	Q92504	-1.48e+00
SAMD4A	Q9UPU9-3	O95429	1.19
SAMHD1	Q9Y3Z3	O75923	3.84
SAP30	O75446	Q16576	1.22
SAT1	Q9H2H9	P24593	1.32
SCD	O00767	P08034	-1.98e+00
SLC22A23	A1A5C7-2	P27352	-1.28e+00
SLC7A14	Q8TBB6	P63027	-2.84e+00
SLC7A6	Q92536	Q9UPQ8	1.64
SMIM3	Q9BZL3	Q9H2H9	1.26
SOCS1	O15524	P46109	-1.15e+00
SORT1	Q99523	P01138	2.21

Input	UniProt Id	Interacts with	#FC
SOX4	Q06945	P04637	-2.38e+00
SQOR	Q9Y6N5	P01106	1.01
STOM	P27105	P50281	1.42
SUN2	Q9UH99	P52292	1.88
SYNPO2	Q9UMS6	Q13418	1.72
TBX18	O95935	Q13077	-1.81e+00
TCEAL4	Q96EI5	Q93009	1.52
TENM4	Q6N022	Q92608	-1.45e+00
TGFB2	P61812	P05067	-1.62e+00
TGFBR2	P37173	Q8IX30	1.44
THBS1	P07996-PRO_0000035842	P16671	1.94
TJP2	Q9UDY2	Q14160	1.97
TMCC2	O75069	P02649	-1.05e+00
TMEM119	EBI-17423904	Q14973	-1.19e+00
TMEM35A	Q53FP2	P07204	-1.67e+00
TNFAIP6	P98066	P10145	-2.50e+00
TNFRSF11B	O00300	Q9Y6Q6	-1.54e+00
TNIK	Q9UKE5	O14920	-1.15e+00
TRIB3	Q96RU7	P18848	-1.10e+00
TSC22D1	Q15714	Q15047	1.18
TSC22D3	Q99576-3	Q9Y6D9	3.32
TUBA1A	Q71U36	Q9Y241	-1.29e+00
TUBA4A	P68366	P30622	-1.45e+00
TUBB	P07437	P05412	-1.21e+00
TUBB3	Q13509	Q5S007	-1.49e+00
TXNRD1	Q16881	Q03135	1.53
UBASH3B	Q8TF42	P29353	1.1
USP53	Q70EK8	P46109	2.3
VCAM1	P19320	P31948	-3.60e+00
VEGFA	P15692-4	P35968, P17948	-1.23e+00
VGLL3	A8MV65-2	Q8TDS5	1.34
WASF3	Q9UPY6-2	P61024	1.08
YIF1B	Q5BJH7	O15354	1.13
ZBTB16	Q05516	P05231	7.05
ZHX3	Q9H4I2	Q9UBE8	1.13

Input	ChEBI Id	Interacts with	#FC
CYTH3	O43739	16618	1.18
DNM1	Q05193	15996	-1.74e+00
FAM20A	Q96MK3	15422	1.09
FGD4	Q96M96	17283	2.26
MX1	P20591	18348	-1.01e+00
PLA2G4A	P47712	18348	-2.45e+00

7. Identifiers not found

These 124 identifiers were not found neither mapped to any entity in Reactome.

10-Mar	AC005674.2	AC007620.2	AC010255.1	AC011611.3	AC012349.1	AC027237.3	AC079467.1
AC090673.1	AC097534.2	AC098847.2	AC138866.2	AFAP1L1	AIF1L	AKAP2	AL035681.1
AL133415.1	AL133453.1	ANGPTL1	ANGPTL7	AP001542.3	C10orf10	C14orf132	C20orf96
C2CD2	CADPS2	CCDC69	CCDC71L	CLIC6	CORO2B	CPA4	CPED1
CRIM1	DANCR	DNM1P47	ENC1	EVA1C	FAIM2	FAM107B	FAM171B
FAM198B	FAM43A	FAM46C	FER1L6	FIBIN	FRZB	GALM	GDF7
GPRC5B	GRAMD2B	GXYLT2	HAPLN3	HSPB3	IGDCC4	IGFLR1	IGSF10
KAZALD1	KCTD12	KIAA1755	KLF9	KLHL23	LBH	LINC00968	LINC02202
LRRC15	LRRC17	MAMDC2	MARCKSL1	MEX3B	MICAL2	MINDY2	MXRA5
NAV3	NEK10	NEXN	NXPH3	NYNRIN	OLFML2A	PAPLN	PHOSPHO2
PKDCC	PLXDC1	PLXDC2	POM121L9P	PRSS35	PXDC1	RAB11FIP1	RASL10B
RASL11B	RASL12	RELL1	RGMB-AS1	RND2	RPL36A-HNRNPH2	RRAD	RTL3
RWDD4	SAMD5	SGCD	SIPA1L2	SLC45A1	SMTNL2	SSH2	STC1
STEAP1	STEAP4	STIM2	STK17B	TAGLN	TCEAL3	TEX2	TIMP4
TLDC2	TM4SF1	TMEM200A	TMEM217	TRNP1	TSPAN11	ULK2	VWCE
WDR63	WFDC1	YPEL4	ZNF821				